Supporting Information

Stepwise assembly and reversible structural transformation of ligated titanium coated bismuth-oxo cores: shell morphology engineering for enhanced chemical fixation of CO_2

Qing-Rong Ding,[a,b] Yinghua Yu,[a] Changsheng Cao,[a] Jian Zhang[a] and Lei Zhang*[a]

[a] State Key Laboratory of Structural Chemistry, Fujian Institute of Research on the Structure of Matter, Chinese Academy of Sciences, Fuzhou, Fujian 350002, P. R. China.

[b] University of Chinese Academy of Sciences, Chinese Academy of Sciences, Beijing 100049, China

E-mail: LZhang@fjirsm.ac.cn

Materials and Methods. All reagents and solvents employed are commercially available and are used as received without further purification. Bismuth subsalicylate was bought from Alfa Aesar. $Ti(O^iPr)_4$ (96%) was bought from Admas-beta. Salicylic acid, piperazine, cis-4-cyclohexene-1,2-dicarboxylic acid, di(trimethylolpropane), 2,2'-biphenol, epichlorohydrin, propylene oxide, 1,2-epoxybutane, styrene oxide, cyclohexene oxide, dibromomethane and chloroform-d were bought from Energy Chemical. The phase purity of products was confirmed by PXRD using a Rigaku Dmax2500 diffractometer with Cu Kα radiation (λ= 1.54056 Å) with a step size of 5°/min. Thermogravimetric analyses (TGA) were performed using a NETSCHZ STA-449C thermoanalyzer with a heating rate of 10°C/min under a nitrogen atmosphere. Fourier transform infrared (FT-IR) spectra were recorded with a Spectrum One FT-IR Spectrometer in the 400-4000 cm^{-1} range. The UV-vis diffuse reflection data were recorded at room temperature using a powder sample with $BaSO_4$ as a standard on a Perkin-Elmer Lambda950 UV-vis spectrophotometer and scanned at 200-800 nm in the reflectance mode with application of the Kubelka-Munk equation, $(F(R) = (1\text{-}R)^2/2R)$,[1] where R representing the reflectance. The solution-state UV-vis absorption spectra of nanoclusters before and after catalytic reaction were recorded using a Perkin-Elmer Lambda365 with 1 nm/s scan rate and scanned at 200-800 nm. The elemental analyses were performed on an EA1110 CHNS-0 CE elemental analyzer. The energy dispersive spectroscopy (EDS) analyses of single crystals were performed on a JEOL JSM6700F field-emission scanning electron microscope equipped with an Oxford INCA system. Inductively coupled plasma (ICP) analyses for Bi and Ti were conducted on an Ultima2 spectrometer. Routine ^1H NMR spectra were recorded on a Bruker AVANCE III (400 MHz for ^1H NMR).

Photocurrent measurement. Films of compounds were prepared by the solution coating method. The crystals (5 mg) were placed in 0.5 mL isopropanol and 10 μL Nafion (5 wt.%) mixed solvent, then the mixture was ultrasonicated for 30 min to achieve a homogeneous ink. The 50 μL solutions were transferred by pipette and then dropped on the cleaned FTO glass (1.5 × 4.0 cm^2, 50 Ω per square cm). The coating film was obtained after evaporation under ambient atmosphere. A 300 W (PLS-SXE300D) Xe lamp with a 420 nm cutoff filter, located 20 cm away from the surface of the FTO electrode, was employed as light source. The photocurrent experiments were performed on a CHI 760e electrochemical workstation (Chenhua, Shanghai, China) in a three-electrode system, with the sample coated FTO glass (1.0 cm × 1.0 cm) as the working electrode, a Pt plate as the auxiliary electrode and an Ag/AgCl electrode as the reference electrode. 40ml aqueous solution of Na_2SO_4 (0.2 mol L^{-1}) was used as the electrolyte solution first. All the tests were performed at the same bias potential of +0.8 V. The lamp was kept on continuously, and a manual shutter was used to block exposure of the sample to the light.

Catalytic reaction. In each reaction, 10 mmol epoxide substrate, 0.005 mmol catalysts, and 1mmol tetra-n-tert-butylammonium bromide (TBAB) were mixed in a 25 mL Schlenk tube. The Schlenk tube was solvent-free and purged with 1 atm CO_2 at room temperature for 24 h or 48 h with 550 rpm stirring. After reaction, the products were collected and analyzed by ^1H NMR (400 MHz, $CDCl_3$) to study its conversion ratio using dibromomethane as an internal standard. The mixed solution after reaction was added to a large amount of ethanol, and further centrifuged to isolate the spent catalyst, which was washed with ethanol several times. After that, the catalyst was reintroduced into the system to restart a new recycle reaction or other characterization.

Synthesis of $[Ti_6Bi_{38}O_{45}(SAC)_{18}(HSAC)_{12}]\cdot 2(H_2O)\cdot 4(NBA)\cdot 11(DMF)$ (PTC-281)
Bismuth subsalicylate (0.362 g, 1.0 mmol), salicylic acid (0.138 g, 1.0 mmol), dimethylformamide (4 ml) and 1-butanol (4 ml) were mixed at room temperature and then dropwise $Ti(O^iPr)_4$ (0.5 ml, 1.6 mmol) was added. The resultant solution was heated at 80 °C for three days in a glass vial with a polyethylene

screw cap, and then cooled to room temperature, yellow rodlike crystals of **PTC-281** were obtained (yield: ~60% based on $Ti(O^iPr)_4$). EA (%) calculated for $C_{259}H_{253}N_{11}O_{152}Ti_6Bi_{38}$ (14180.26): C, 21.94; H, 1.80; N, 1.09. Found: C, 21.65; H, 1.62; N, 1.21. FT-IR (KBr pellet, cm^{-1}): 3446(w) 2952(w) 1595(s) 1453(s) 1375(s) 1347(s) 1243(m) 1137(m) 1041(w) 890(m) 829(w) 758(m) 706(w) 669(w) 640(w) 546(s).

Synthesis of $H_2[Ti_{14}Bi_{38}O_{50}(SAC)_{30}(EtO)_{12}]\cdot 12(DMF)$ (PTC-282)

PTC-281 (0.200 g), salicylic acid (0.276 g, 2.0 mmol), piperazine (0.086 g, 0.1 mmol), dimethylformamide (4 ml) and ethyl acetate (4 ml) were mixed at room temperature and then dropwise $Ti(O^iPr)_4$ (0.5 ml, 1.6 mmol) was added. The resultant solution was heated at 80 °C for one night in a glass vial with a polyethylene screw cap, and then cooled to room temperature, yellow block crystals of **PTC-282** were obtained. EA (%) calculated for $C_{270}H_{266}N_{12}O_{164}Ti_{14}Bi_{38}$ (14914.37): C, 21.74; H, 1.80; N, 1.13. Found: C, 21.87; H, 1.64; N, 1.23. FT-IR (KBr pellet, cm^{-1}): 1648(s) 1595(s) 1533(w) 1455(s) 1344(s) 1239(m) 1140(w) 1103(w) 1099(w) 1032(w) 887(m) 834(m) 763(m) 706(w) 672(w) 639(w) 589(w) 456(w).

Synthesis of $[Ti_{16}Bi_{38}O_{51}(SAC)_{28}(HSAC)_2(DEA)_4(PhO)_{10}]\cdot 2(CH_3CN)$ (PTC-283)

PTC-281 (0.200 g), salicylic acid (0.138 g, 2.0 mmol), acetonitrile (4 ml) and phenol (4 ml) were mixed at room temperature and then diethanolamine (30 μL, 0.3 mmol), $Ti(O^iPr)_4$ (0.5 ml, 1.6 mmol) were added. The resultant solution was heated at 80 °C for one night in a glass vial with a polyethylene screw cap, and then cooled to room temperature, yellow block crystals of **PTC-283** were obtained. EA (%) calculated for $C_{290}H_{210}N_6O_{159}Ti_{16}Bi_{38}$ (15030.27): C, 23.17; H, 1.41; N, 0.56. Found: C, 23.31; H, 1.34; N, 0.63. FT-IR (KBr pellet, cm^{-1}): 1642(w) 1597(s) 1533(w) 1455(s) 1344(s) 1236(m) 1140(w) 1103(w) 1033(w) 892(m) 838(m) 759(w) 706(w) 680(w) 643(w) 527(w) 456(w).

Synthesis of $[Ti_{16}Bi_{38}O_{44}(SAC)_{34}(DPC)_6(PhO)_8]\cdot 4(CH_3CN)$ (PTC-284)

PTC-281 (0.200 g), salicylic acid (0.138 g, 2.0 mmol), cis-4-cyclohexene-1,2-dicarboxylic acid (0.068 g, 0.4 mmol), acetonitrile (4 ml) and phenol (4 ml) were mixed at room temperature and then dropwise $Ti(O^iPr)_4$ (0.5 ml, 1.6 mmol) was added. The resultant solution was heated at 80 °C for one night in a glass vial with a polyethylene screw cap, and then cooled to room temperature, red spininess crystals of **PTC-284** were obtained. EA (%) calculated for $C_{342}H_{236}N_4O_{178}Ti_{16}Bi_{38}$ (15956.97): C, 25.74; H, 1.49; N, 0.35. Found: C, 25.81; H, 1.40; N, 0.28. FT-IR (KBr pellet, cm^{-1}): 1642(w) 1597(s) 1575(s) 1522(w) 1455(s) 1343(m) 1236(s) 1140(w) 1028(w) 892(m) 838(m) 759(m) 705(w) 672(w) 643(w) 585(w) 527(w).

Synthesis of $[Ti_{18}Bi_{38}O_{50}(SAC)_{24}(DTPP)_6(DMT)_6][O^iPr]_2\cdot 12(DMF)$ (PTC-285)

PTC-281 (0.200 g), salicylic acid (0.138 g, 2.0 mmol), di(trimethylolpropane) (0.250 g, 2.0 mmol), 2,2'-biphenol (0.068 g, 0.4 mmol), dimethylformamide (4 ml) and n-propanol (4 ml) were mixed at room temperature and then dropwise $Ti(O^iPr)_4$ (0.5 ml, 1.6 mmol) was added. The resultant solution was heated at 80 °C for one night in a glass vial with a polyethylene screw cap, and then cooled to room temperature, orange cube crystals of **PTC-285** were obtained. EA (%) calculated for $C_{354}H_{374}N_{12}O_{178}Ti_{18}Bi_{38}$ (16444.38): C, 25.85; H, 2.29; N, 1.02. Found: C, 25.78; H, 2.30; N, 1.12. FT-IR (KBr pellet, cm^{-1}): 1605(s) 1579(s) 1575(s) 1543(w) 1460(s) 1348(s) 1277(w) 1244(s) 1140(m) 1079(s) 1031(w) 957(w) 892(m) 834(m) 706(w) 676(w) 643(w) 539(w) 457(w).

Synthesis of $H_2[Ti_{20}Bi_{38}O_{50}(SAC)_{30}(DTPP)_6(CH_3O)_{12}]\cdot 4(DMF)$ (PTC-286)

PTC-281 (0.200 g), salicylic acid (0.138 g, 2.0 mmol), di(trimethylolpropane) (0.250 g, 2.0 mmol), dimethylformamide (4 ml) and methanol (4 ml) were mixed at room temperature and then dropwise $Ti(O^iPr)_4$ (0.5 ml, 1.6 mmol) was added. The resultant solution was heated at 80 °C for one night in a glass vial with a polyethylene screw cap, and then cooled to room temperature, yellow block crystals of

PTC-286 were obtained. EA (%) calculated for $C_{306}H_{318}N_4O_{186}Ti_{20}Bi_{38}$ (15926.30): C, 23.08; H, 2.02; N, 0.35. Found: C, 23.22; H, 2.11; N, 0.43. FT-IR (KBr pellet, cm^{-1}): 3427(w) 3066(w) 2960(w) 2855(w) 1600(s) 1579(s) 1547(w) 1460(s) 1343(s) 1238(m) 1140(m) 1079(w) 1028(w) 954(w) 892(m) 834(m) 706(w) 676(w) 643(w) 539(w) 457(w).

General Methods for X-ray Crystallography. Crystallographic data of **PTC-281** to **286** were collected on ROD diffractometer which is equipped with a gallium micro-focus metaljet X-ray sources (λ = 1.3405 Å) at 100 K. The structures were solved with the dual-direct methods using *ShelxT* and refifined with the full-matrix least-squares technique based on F^2 using the *SHELXL*-2014[2] program package and Olex-2[3] software. Non-hydrogen atoms were refined anisotropically, and all hydrogen atoms bond C were generated geometrically. Some disordered solvent molecules are removed by using the SQUEEZE[4] routine of PLATON.[5] The details of the SQUEEZE corrections, including the volume of void space and electron counts, are provided in the cif file. The cluster core of **PTC-285** is a +2 cation. According to the reactants added in the synthesis of **PTC-285** and also the elemental analysis results, we speculate that the peripheral counter anions are two free O^iPr groups in the cavity. Unfortunately, due to the weak diffraction, these counter anions could not be crystallographically defined. The X-ray crystallographic coordinates for structures reported in this article have been deposited at the Cambridge Crystallographic Data Centre (CCDC) under deposition numbers CCDC 2104507, 2104508, and 2104511 to 2104515 for **PTC-281**, **PTC-281R**, and **PTC-282** to **PTC-286**. These data can be obtained free of charge from the Cambridge Crystallographic Data Centre via http://www.ccdc.cam.ac.uk/data_request/cif.

(1) W. W. Wendlandt, H. G. Hecht, *Interscience publishers: New York*, 1966, **46**, 593.

(2) D. Leggas, O. V. Tsodikov, *Acta Crystallogr A Found Adv*. 2015, **71**, 319-324.

(3) O. V. Dolomanov, L. J. Bourhis, R. J. Gildea, J. A. K Howard, H. Puschmann, *J. Appl. Crystallogr*. 2009, **42**, 339-341.

(4) A. L. Spek, *Acta Crystallogr C Struct Chem*. 2015, **71**, 9-18.

(5) A. L. Spek, *Acta Crystallogr. D Biol. Crystallogr*. 2009, **65**, 148-155.

Table S1. Crystallographic data and structure refinement summary for **PTC-281** and **PTC-282**

	PTC-281	**PTC-281R**	**PTC-282**
Cryst. formula	$C_{254}H_{244}N_{11}O_{149}Ti_6Bi_{38}$	$C_{240}H_{202}N_{10}O_{145}Ti_6Bi_{38}$	$C_{252}H_{222}N_6O_{158}Ti_{14}Bi_{38}$
M_r	14063.23	13774.74	14474.18
T/K	100.4(7)	104.2(3)	99.97(11)
Crystal system	Triclinic	Monoclinic	Trigonal
Space group	*P*-1	*C*2/*c*	*R*-3*c*
a/Å	23.6421(2)	31.6643(3)	24.8265(5)
b/Å	23.6421(2)	33.3838(3)	24.8265(5)
c/Å	38.8128(3)	35.4595(3)	120.4773(15)
α (°)	107.5720(10)	90	90
β (°)	91.1110(10)	91.5690(10)	90
γ (°)	114.4930(10)	90	120
V/Å^3	18711.2(3)	37469.3(6)	64308(3)
Z	2	4	6
Dc/mg m^{-3}	2.496	2.442	2.242
μ/mm^{-1}	25.023	24.973	22.612
Indep reflns $[I>2\sigma(I)]$	64356	33048	12593
F(000)	12646.0	24632.0	39012.0
GOF	1.072	1.029	1.069
CCDC No.	2104507	2104508	2104511
R_1[a], wR_2[b] $[I>2\sigma(I)]$	0.0493, 0.1277	0.0866, 0.2288	0.0831, 0.2302
R_1[a], wR_2[b] (all data)	0.0602, 0.1333	0.0946, 0.2414	0.0966, 0.2439

[a] $R_1 = \Sigma(||F_o| - |F_c||)/\Sigma|F_o|$. [b] $wR_2 = [\Sigma w(|F_o|^2 - |F_c|^2)^2/\Sigma w(F_o^2)]^{1/2}$.

Table S2. Crystallographic data and structure refinement summary for **PTC-283** to **PTC-285**

	PTC-283	**PTC-284**	**PTC-285**
Cryst. formula	$C_{290}H_{210}N_6O_{159}Ti_{16}Bi_{38}$	$C_{342}H_{236}N_4O_{178}Ti_{16}Bi_{38}$	$C_{312}H_{276}O_{164}Ti_{18}Bi_{38}$
M_r	15030.27	15956.97	15452.75
T/K	110.01(10)	100.00(14)	100.01(11)
Crystal system	Monoclinic	Monoclinic	Trigonal
Space group	$P2_1/n$	$I2/a$	R-3
a/Å	22.5953(2)	25.2403(1)	39.6442(16)
b/Å	37.4685(3)	43.6932(2)	39.6442(16)
c/Å	23.2719(2)	49.0721(3)	23.6456(15)
α (°)	90	90	90
β (°)	98.1640(10)	96.6720(10)	90
γ (°)	90	90	120
V/Å^3	19502.6(3)	53751.6(5)	32184(3)
Z	2	4	3
Dc/mg m^{-3}	2.559	1.972	2.392
μ/mm^{-1}	25.087	18.253	23.008
indep reflns $[I>2\sigma(I)]$	34364	46869	12486
F(000)	13540.0	28984.0	21030.0
GOF	1.044	1.018	1.217
CCDC No.	2104512	2104513	2104514
R_1[a], wR_2[b] $[I>2\sigma(I)]$	0.0635, 0.1590	0.0669, 0.1720	0.1020, 0.3013
R_1[a], wR_2[b] (all data)	0.0798, 0.1733	0.0896, 0.1947	0.1275, 0.3285

[a] $R_1 = \Sigma(||F_o| - |F_c||)/\Sigma|F_o|$. [b] $wR_2 = [\Sigma w(|F_o|^2 - |F_c|^2)^2/\Sigma w(F_o^2)]^{1/2}$.

Table S3. Crystallographic data and structure refinement summary for **PTC-286**

	PTC-286
Cryst. formula	$C_{306}H_{304}N_4O_{186}Ti_{20}Bi_{38}$
M_r	15912.75
T/K	100.01(10)
Crystal system	Triclinic
Space group	*P*-1
a/Å	23.1533(5)
b/Å	23.5480(5)
c/Å	23.6018(5)
α (°)	117.688(2)
β (°)	115.545(2)
γ (°)	92.2502(17)
V/Å^3	9807.4(4)
Z	1
Dc/mg m^{-3}	2.694
μ/mm^{-1}	25.420
indep reflns $[I > 2\sigma(I)]$	34316
F(000)	7250.0
GOF	1.037
CCDC No.	2104515
R_1[a], wR_2[b] $[I > 2\sigma(I)]$	0.0632, 0.1615
R_1[a], wR_2[b] (all data)	0.0936, 0.1971

[a] $R_1 = \Sigma(||F_o| - |F_c||)/\Sigma|F_o|$. [b] $wR_2 = [\Sigma w(|F_o|^2 - |F_c|^2)^2/\Sigma w(F_o^2)]^{1/2}$.

Table S4. Bond valence sum (BVS) analysis of titanium and bridged oxygen atoms[a] for **PTC-281** to **286**

PTC-281								
Ti1 4.255			Ti2 4.231			Ti3 4.315		
Ti1-O030	d=1.997(12)	0.611	Ti2-O037	d=2.010(11)	0.590	Ti3-O02D	d=2.041(10)	0.542
Ti1-O03B	d=2.014(12)	0.584	Ti2-O03S	d=1.976(11)	0.647	Ti3-O02E	d=1.890(10)	0.816
Ti1-O03C	d=2.025(12)	0.566	Ti2-O047	d=1.905(12)	0.784	Ti3-O02J	d=1.992(9)	0.619
Ti1-O03N	d=1.890(14)	0.816	Ti2-O04G	d=2.012(11)	0.587	Ti3-O02W	d=1.861(10)	0.883
Ti1-O03X	d=1.891(12)	0.814	Ti2-O04K	d=1.893(12)	0.809	Ti3-O02X	d=1.871(11)	0.859
Ti1-O04I	d=1.869(13)	0.864	Ti2-O04U	d=1.891(12)	0.814	Ti3-O032	d=2.006(9)	0.596
Ti4 4.280			Ti5 4.283			Ti6 4.264		
Ti4-O03Z	d=1.988(12)	0.626	Ti5-O02F	d=2.012(10)	0.587	Ti6-O02H	d=1.988(11)	0.626
Ti4-O041	d=1.998(12)	0.609	Ti5-O02O	d=1.858(10)	0.890	Ti6-O02K	d=1.873(13)	0.854
Ti4-O043	d=1.884(15)	0.829	Ti5-O02S	d=2.026(10)	0.565	Ti6-O02M	d=2.026(11)	0.565
Ti4-O044	d=2.044(12)	0.538	Ti5-O02U	d=1.875(10)	0.850	Ti6-O02T	d=1.891(12)	0.814
Ti4-O04A	d=1.866(14)	0.871	Ti5-O02Z	d=2.010(10)	0.590	Ti6-O02Y	d=2.008(12)	0.593
Ti4-O04M	d=1.894(14)	0.807	Ti5-O03O	d=1.897(11)	0.801	Ti6-O03W	d=1.892(12)	0.812
PTC-282								
Ti1 4.716			Ti2 4.120			Ti3 4.241		
Ti1-O00Q	d=1.948(19)	0.663	Ti2-O00J	d=1.881(15)	0.836	Ti3-O00J	d=1.827(15)	0.929
Ti1-O00Q	d=1.948(19)	0.663	Ti2-O00T	d=2.103(15)	0.459	Ti3-O00L=K	d=1.890(17)	0.779
Ti1-O00Q	d=1.948(19)	0.663	Ti2-O00U	d=1.955(17)	0.684	Ti3-O00L	d=1.92(2)	0.752
Ti1-O00W	d=1.83(2)	0.909	Ti2-O00X	d=1.945(19)	0.703	Ti3-O00P	d=2.016(13)	0.560
Ti1-O00W	d=1.83(2)	0.909	Ti2-O00Y	d=1.85(2)	0.909	Ti3-O00V	d=1.906(16)	0.590
Ti1-O00W	d=1.83(2)	0.909	Ti2-O00Z	d=2.05(2)	0.529	Ti3-O00Z	d=1.985(16)	0.631
PTC-283								
Ti1 4.325			Ti2 4.181			Ti3 4.392		
O00S	1.903(11)	0.788	O014	1.926(11)	0.740	O016	1.876(14)	0.848
O00U	2.078(11)	0.491	O01D	1.948(13)	0.698	O01L	1.996(12)	0.613
O00Z	2.103(11)	0.459	O01P	2.015(11)	0.582	O01O	2.042(14)	0.541
O013	1.953(11)	0.688	O01S	2.030(14)	0.559	O01R	2.002(12)	0.603
O01I	1.748(12)	1.198	O028	1.705(11)	1.346	O02A	1.860(14)	0.885

O01J	1.946(12)	0.701	N02C	2.318(13)	0.256	O02E	1.853(15)	0.902
Ti4 4.198			Ti5 4.446			Ti6 4.227		
O02J	1.917(16)	0.759	O02P	2.054(18)	0.524	O01H	2.015(14)	0.582
O02Y	1.87(2)	0.861	O02Q	1.82(2)	0.934	O01W	2.023(14)	0.569
O03D	1.793(19)	1.061	O03D	1.930(18)	0.679	O01X	1.926(13)	0.740
O03K	2.031(17)	0.557	O03Q	1.83(2)	0.909	O021	1.918(13)	0.757
O58	1.83(2)	0.960	O048	2.122(19)	0.414	O02F	1.714(12)	1.313
			O16	1.69(2)	0.986	N02L	2.304(15)	0.266
Ti7 4.322			Ti8 4.232					
O01C	1.863(14)	0.878	O01B	1.861(14)	0.883			
O01F	1.843(14)	0.927	O01G	1.848(13)	0.914			
O01Q	2.024(12)	0.568	O01T	1.875(13)	0.850			
O01Z	1.862(14)	0.880	O01U	2.038(12)	0.547			
O023	2.067(12)	0.506	O025	2.054(12)	0.524			
O02I	2.027(14)	0.563	O02K	2.061(13)	0.514			
PTC-284								
Ti1 4.006			Ti2 4.291			Ti3 4.330		
Ti1-O01T	d=1.857(13)	0.892	Ti2-O01E	d=2.070(13)	0.484	Ti3-O02C	d=2.042(12)	0.541
Ti1-O01V	d=2.048(12)	0.165	Ti2-O01K	d=2.041(11)	0.527	Ti3-O01B	d=1.848(12)	0.914
Ti1-O01W	d=1.971(13)	0.655	Ti2-O01L	d=1.860(13)	0.854	Ti3-O021	d=2.030(11)	0.559
Ti1-O01Z	d=1.863(12)	0.878	Ti2-O01M	d=1.995(12)	0.595	Ti3-O029	d=1.860(12)	0.885
Ti1-O026	d=2.051(12)	0.528	Ti2-O020	d=1.879(13)	0.812	Ti3-O02H	d=1.868(14)	0.866
Ti1-O02P	d=1.860(14)	0.885	Ti2-O02C	d=1.794(14)	1.019	Ti3-O02M	d=2.026(13)	0.565
Ti4 4.300			Ti5 4.310			Ti6 4.334		
Ti4-O018	d=2.046(12)	0.535	Ti5-O00Z	d=1.848(12)	0.914	Ti6-O02Q	d=2.007(13)	0.574
Ti4-O01R	d=1.843(13)	0.927	Ti5-O01A	d=2.082(11)	0.485	Ti6-O02Z	d=1.976(16)	0.619
Ti4-O024	d=1.951(13)	0.692	Ti5-O01F	d=1.842(12)	0.929	Ti6-O032	d=1.860(14)	0.852
Ti4-O027	d=1.980(11)	0.640	Ti5-O01N	d=1.991(11)	0.621	Ti6-O03N	d=2.073(14)	0.479
Ti4-O02A	d=1.855(12)	0.897	Ti5-O01Q	d=1.849(12)	0.912	Ti6-O03S	d=1.821(17)	0.939
Ti4-O02F	d=1.998(12)	0.609	Ti5-O038	d=2.111(12)	0.449	Ti6-O04R	d=1.850(16)	0.871
Ti7 4.290			Ti8 3.093					

Ti7-O02N	d=2.026(15)	0.542	Ti8-O02V	d=1.983(14)	0.595			
Ti7-O02R	d=1.887(17)	0.786	Ti8-O033	d=2.011(14)	0.551			
Ti7-O02X	d=2.056(15)	0.500	Ti8-O03I	d=1.851(17)	0.850			
Ti7-O030	d=1.989(17)	0.596	Ti8-O04U	d=1.960(15)	0.633			
Ti7-O066	d=1.85(2)	0.861	Ti8-O05W	d=2.075(13)	0.464			
Ti7-O3AA	d=1.795(18)	1.005						
PTC-285								
Ti1 4.719			Ti2 4.385			Ti3 4.386		
O00P	1.96(2)	0.640	O00I	1.736(17)	1.182	O00K	1.973(16)	0.624
O00S	2.01(2)	0.559	O00J	1.854(19)	0.854	O00T	1.90(2)	0.752
O00V	2.053(19)	0.499	O00Q	1.866(17)	0.832	O00Y	1.994(17)	0.588
O017	1.76(2)	1.099	O00W	2.260(18)	0.300	O010	1.964(18)	0.636
O01A	1.83(2)	0.909	O00Y	1.964(16)	0.640	O011	1.88(3)	0.773
O0AA	1.78(3)	1.013	O010	2.001(17)	0.577	O012	1.78(3)	1.013

[a] $V_i=\Sigma S_{ij} = \Sigma\exp[(r_1-r_{ij})/B]$, where r_0 is the length of a single bond (here r1=1.815 for Ti^{IV}-O, r1=1.791 for Ti^{III}-O), r_1 is the bond length between atoms *i* and *j*; B is a constant, the "universal parameter" ~0.37 Å; S_{ij} is the valence of a bond between atoms *i* and *j*; V_i is the sum of all bond valences of the bonds formed by a given atom *i*.

Table S5. The summary of ICP-AES results

	Ti (%)		Bi (%)		Ti / Bi	
	Calculated	Found	Calculated	Found	Calculated	Found
PTC-281	2.03	2.00	56.00	56.03	6	6.25
PTC-282	4.49	4.52	53.25	52.39	14	14.31
PTC-283	5.10	5.04	52.84	51.53	16	16.23
PTC-284	4.80	4.44	49.77	45.86	16	16.06
PTC-285	5.24	5.43	48.28	49.26	18	18.29
PTC-286	6.01	5.88	49.86	47.87	20	20.38

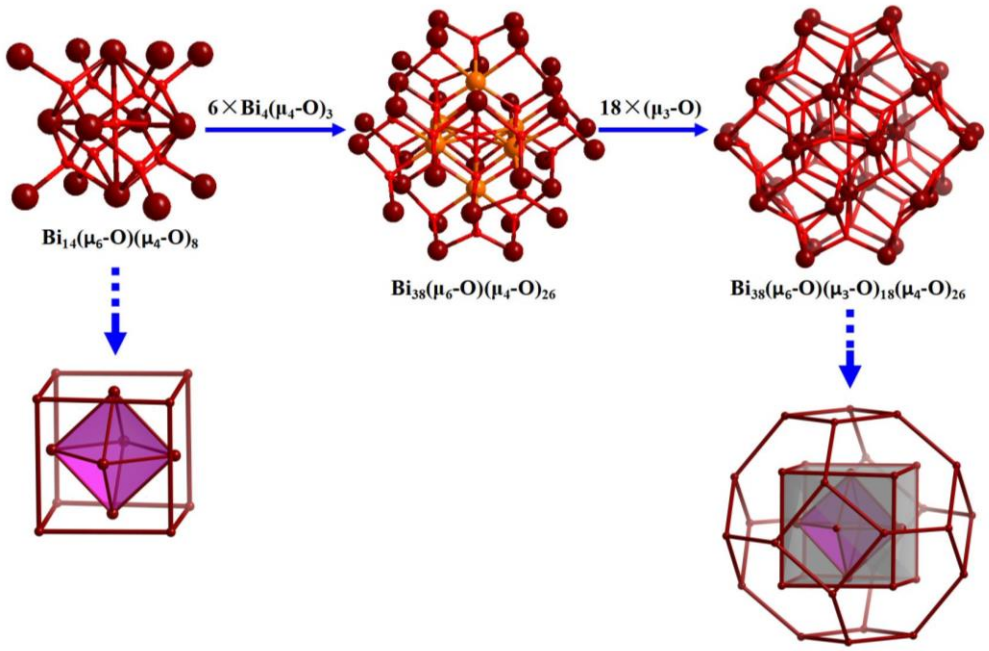

Figure S1. Structural illustration of $Bi_{38}O_{45}$ cluster core in **PTC-281**.

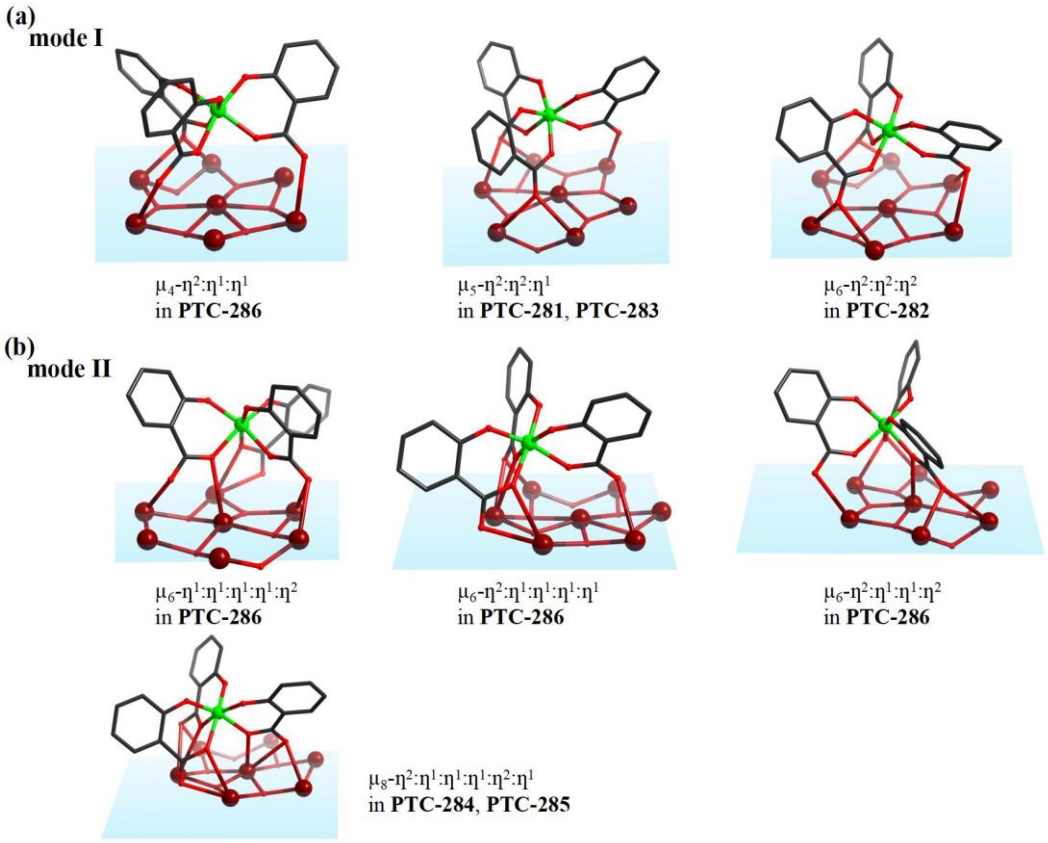

Figure S2. The coordination modes of the $[Ti(SAC)_3]$ metalloligands in all complexes.

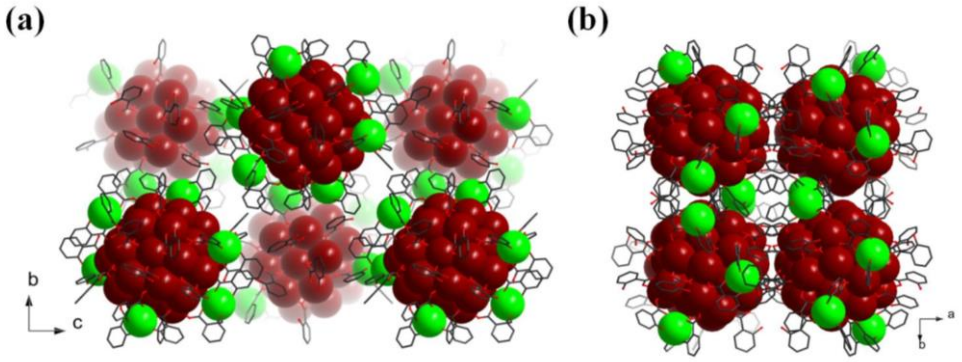

Figure S3. The packing view of **PTC-281** along the a and c-axis. All the H atoms are omitted for clarity. Color codes: green Ti; dark red Bi; black C; red O.

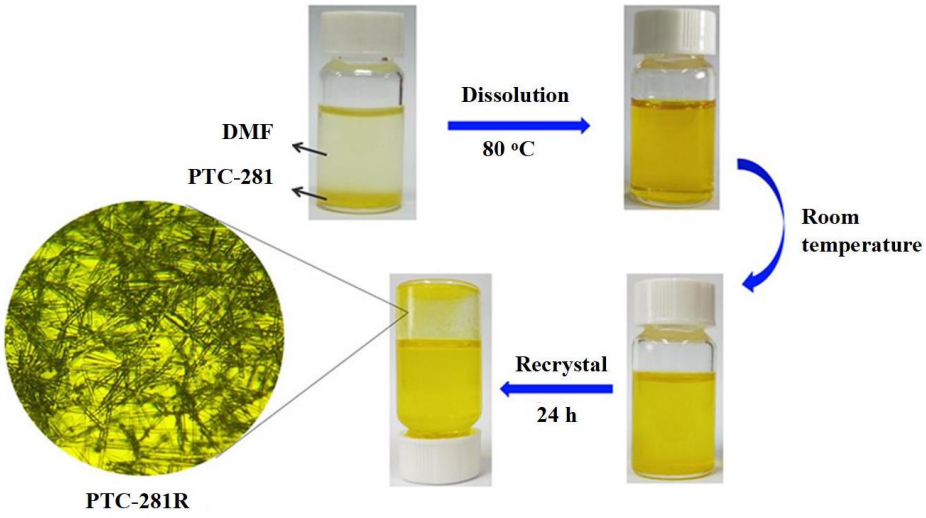

Figure S4. Illustration of the recrystallization process of **PTC-281** to generate **PTC-281R**. 50 mg **PTC-281** and 4 ml DMF were mixed at room temperature, then the resultant solution was heated at 80 °C for 24 h to get a yellow solution. After cooling to room temperature, yellow rod-like crystals were obtained in one day.

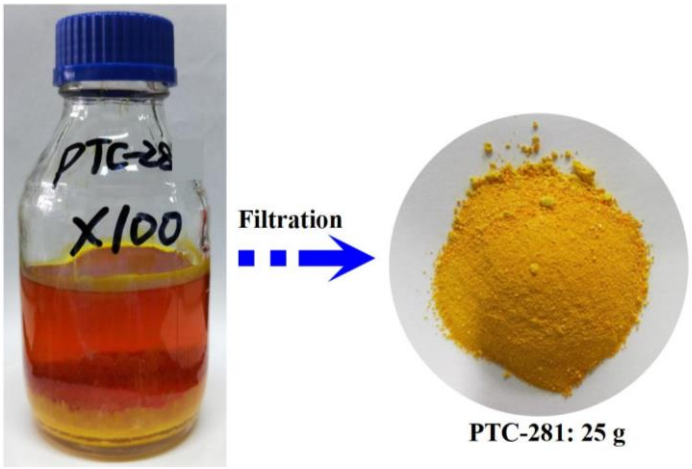

Figure S5. Scaling up synthesis of **PTC-281**. Bismuth subsalicylate (36.2 g), salicylic acid (13.8 g), dimethylformamide (150 ml) and 1-butanol (150 ml) were mixed at room temperature and then dropwise $Ti(O^iPr)_4$ (10 ml) was added. The resultant solution was heated at 80 °C for three days, yellow rod-like crystals of **PTC-281** were obtained.

2

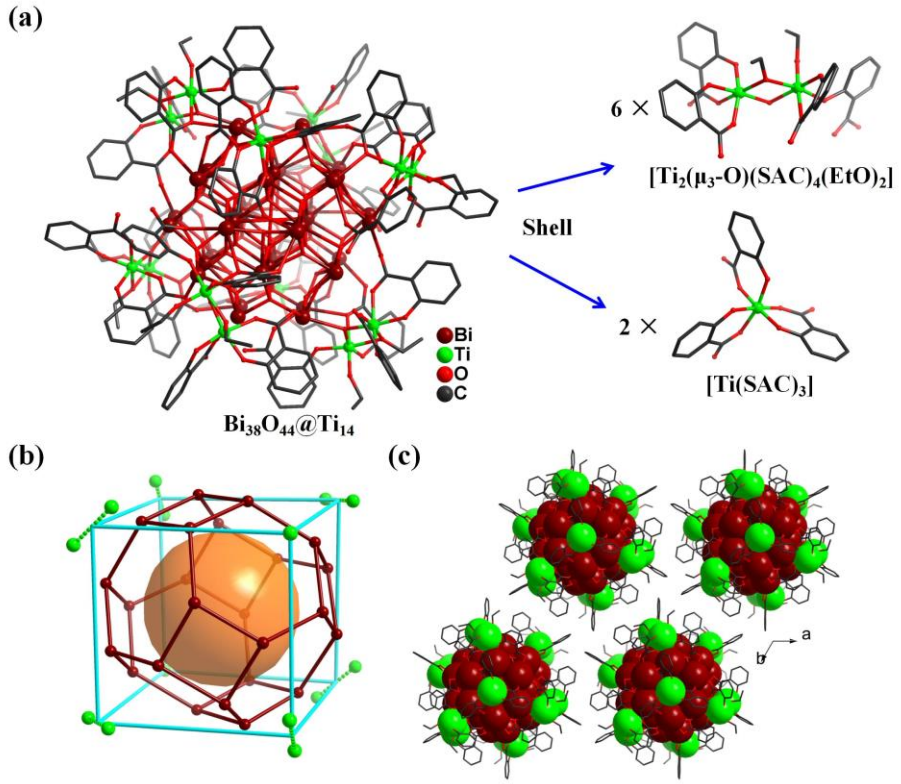

Figure S6. (a) The core-shell structure of **PTC-282**, the shell is made up of six $[Ti_2(\mu_3\text{-}O)(SAC)_4(EtO)_2]$ units and two $[Ti(SAC)_3]$ metalloligands; (b) fourteen titanium atoms form a square cage; (c) the packing view of **PTC-282** along the c-axis. Color codes: green Ti; dark red Bi; black C; red O.

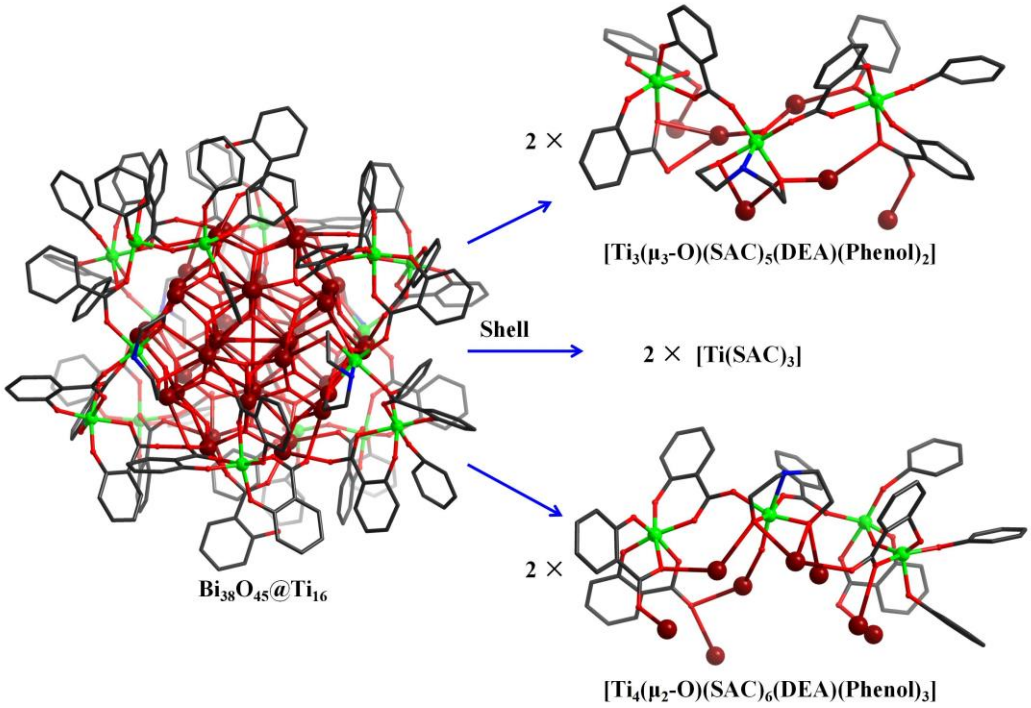

Figure S7. (a) The core-shell structure of **PTC-283**, the shell is made up of two $[Ti_3(\mu_3\text{-}O)(SAC)_5(DEA)_2(Phenol)_2]$ units, two $[Ti_4(\mu_2\text{-}O)(SAC)_6((DEA)(Phenol)_3]$ units and two $[Ti(SAC)_3]$ metalloligands. Color codes: green Ti; dark red Bi; black C; red O.

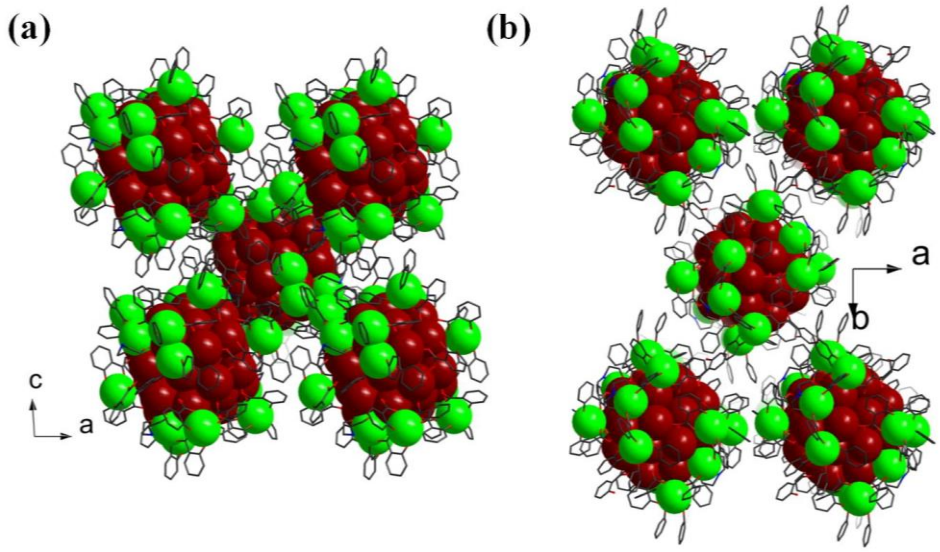

Figure S8. The packing view of **PTC-283** along the b and c-axis. Color codes: green Ti; dark red Bi; black C; red O.

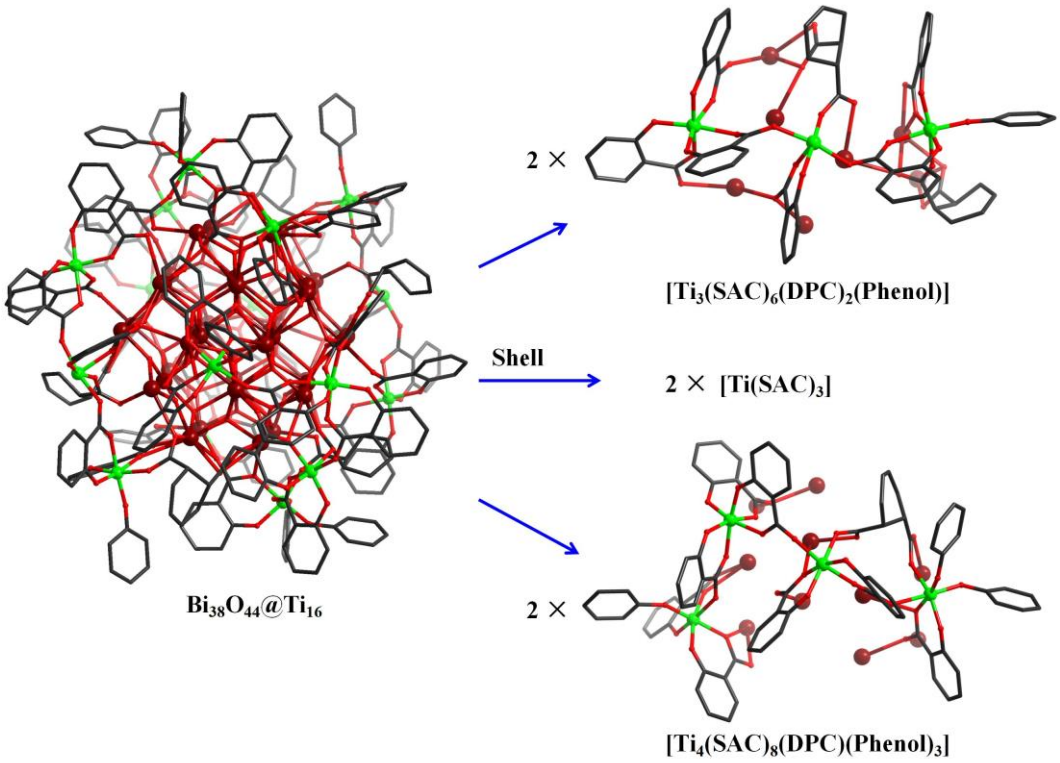

Figure S9. (a) The core-shell structure of **PTC-284**, the shell is made up of two $[Ti_3((SAC)_6(DPC)_2(Phenol)]$ units, two $[Ti_4(SAC)_8((DPC)(Phenol)_3]$ units and two $[Ti(SAC)_3]$ metalloligands. Color codes: green Ti; dark red Bi; black C; red O.

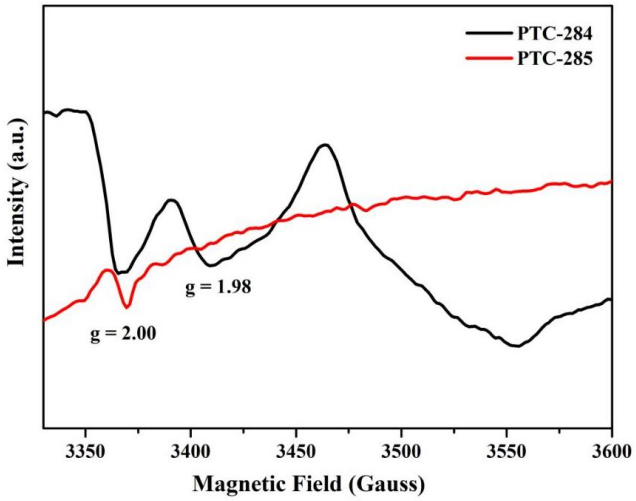

Figure S10. ESR spectra of **PTC-284** and **PTC-285.**

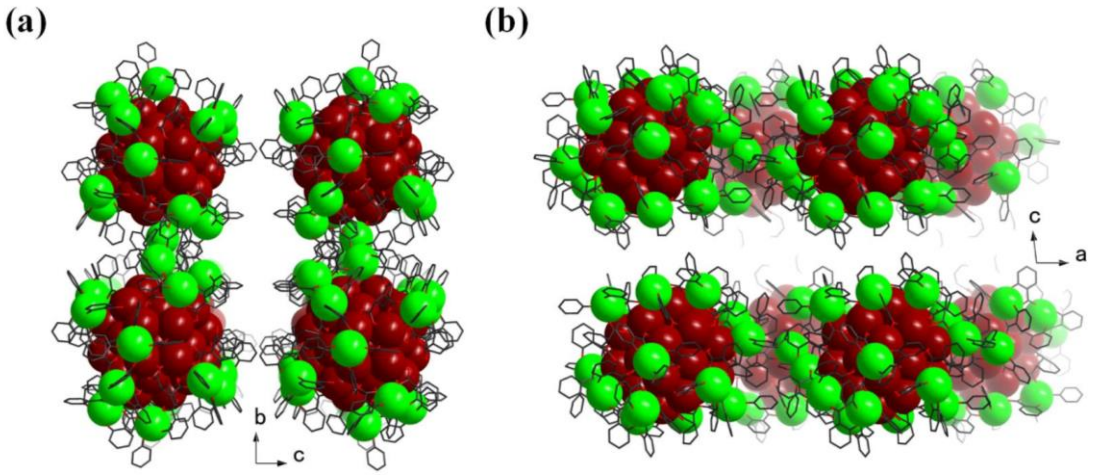

Figure S11. The packing view of **PTC-284** along the a and b-axis. Color codes: green Ti; dark red Bi; black C; red O.

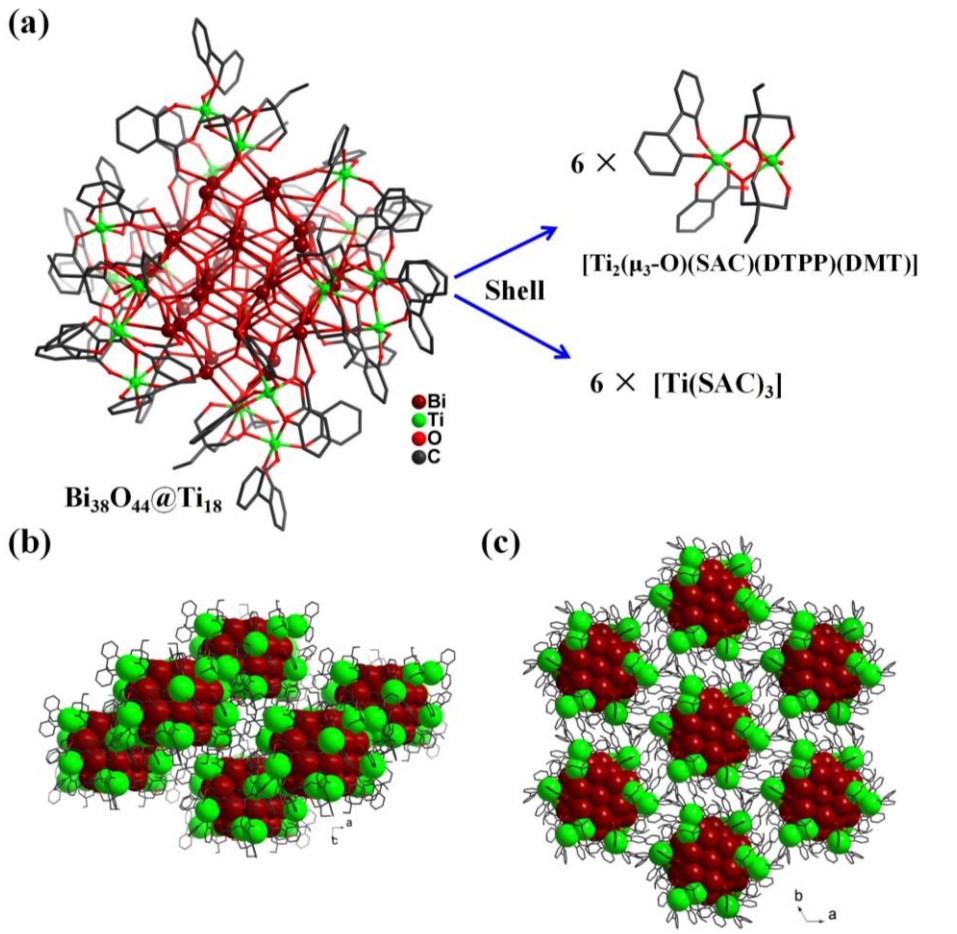

Figure S12. (a) The core-shell structure of **PTC-285**, the shell is made up of six $[Ti_2(\mu_3\text{-}O)(SAC)(DTPP)(DMT)]$ units and six $[Ti(SAC)_3]$ metalloligands; (b) and (c) the packing view of **PTC-285** along the b and c-axis.

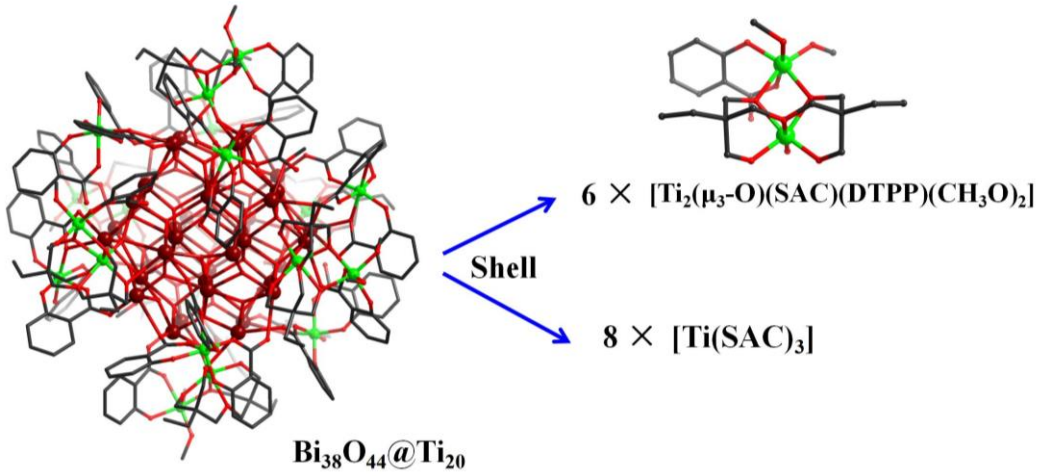

Figure S13. The core-shell structure of **PTC-286**, the shell is made up of six $[Ti_2(\mu_3\text{-}O)(SAC)(DTPP)(CH_3O)_2]$ units and eight $[Ti(SAC)_3]$ metalloligands.

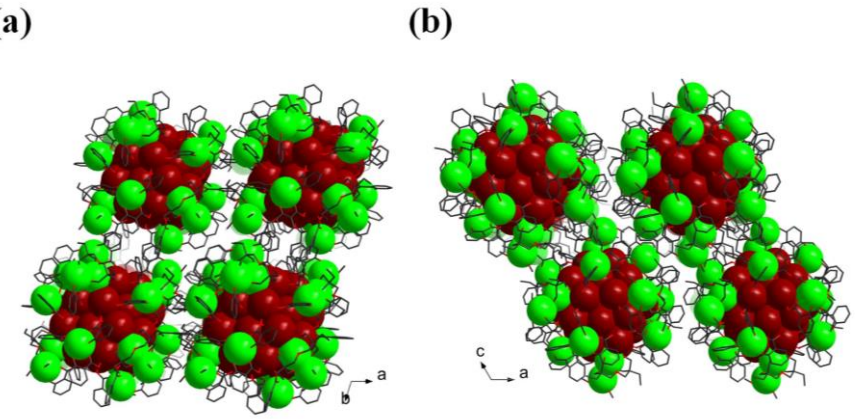

Figure S14. The packing view of **PTC-286** along the c- and b- axis. Color codes: green Ti; dark red Bi; black C; red O.

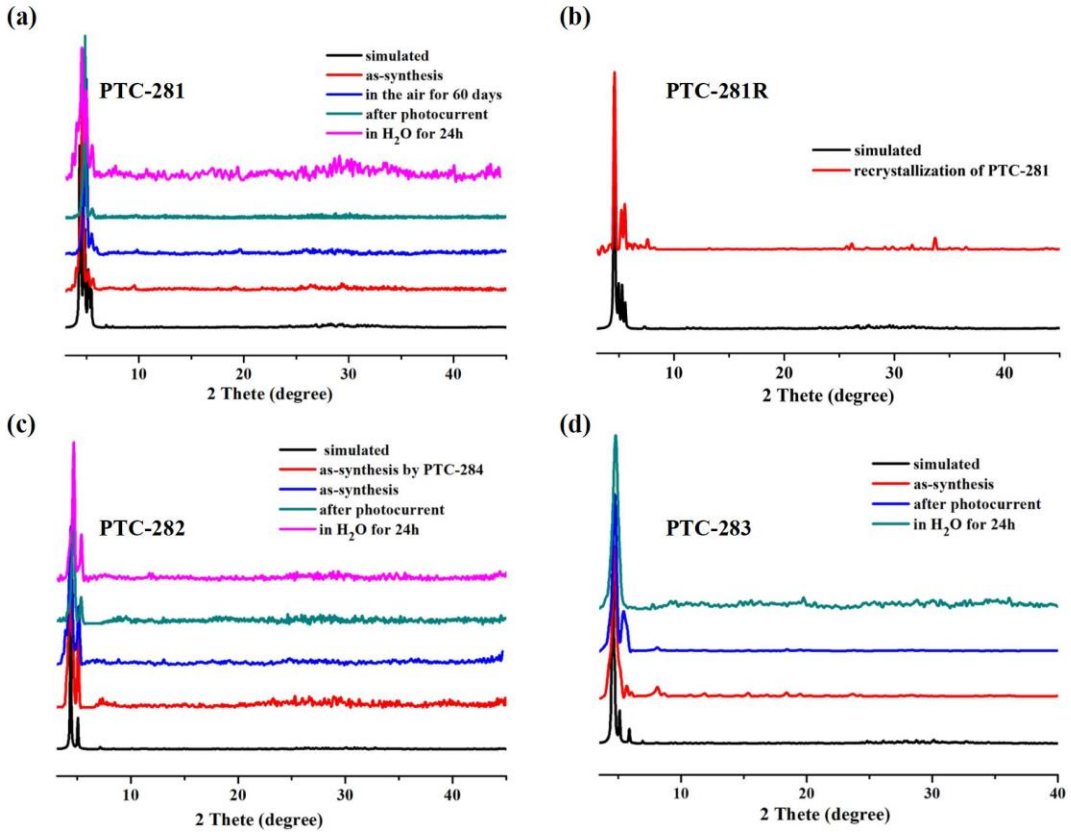

Figure S15. The simulated and experimental PXRD patterns for **PTC-281** to **PTC-283**.

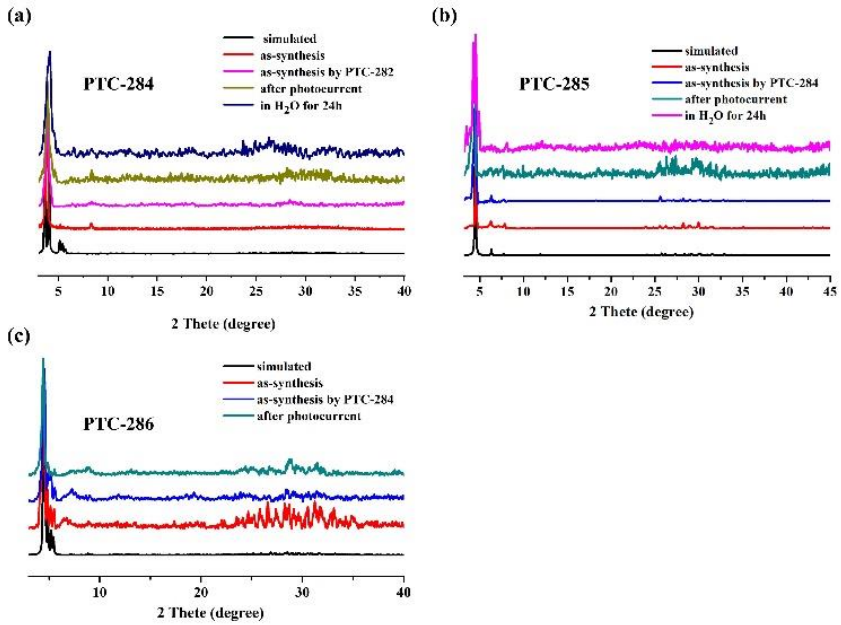

Figure S16. The simulated and recrystallization PXRD patterns for **PTC-284** to **PTC-286**.

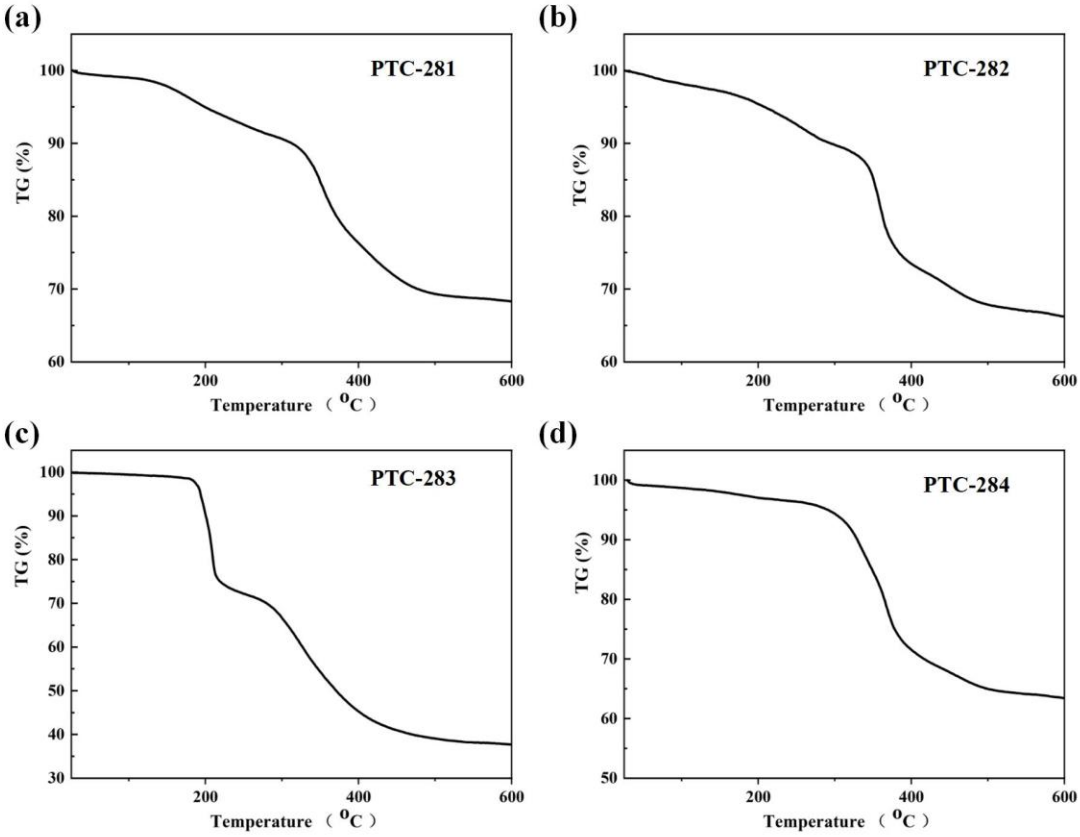

Figure S17. TGA curves of **PTC-281** to **PTC-284**.

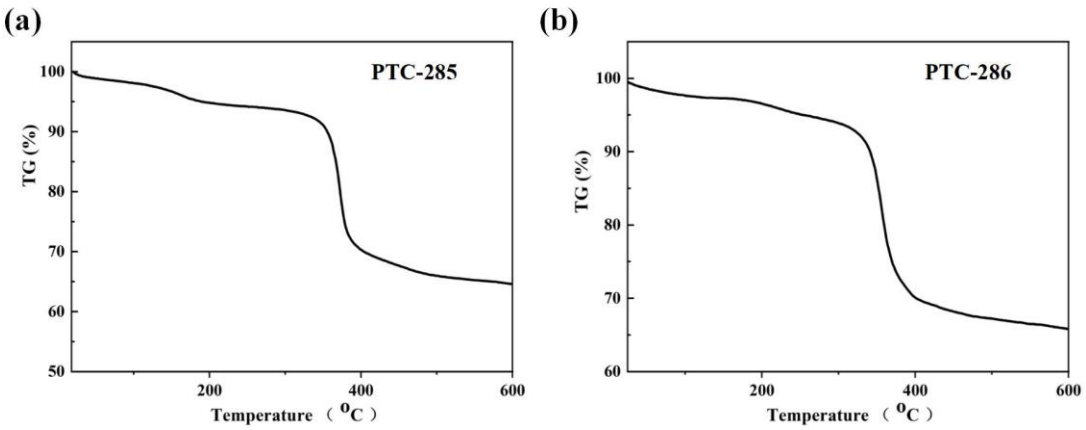

Figure S18. TGA curves of **PTC-285** and **PTC-286.**

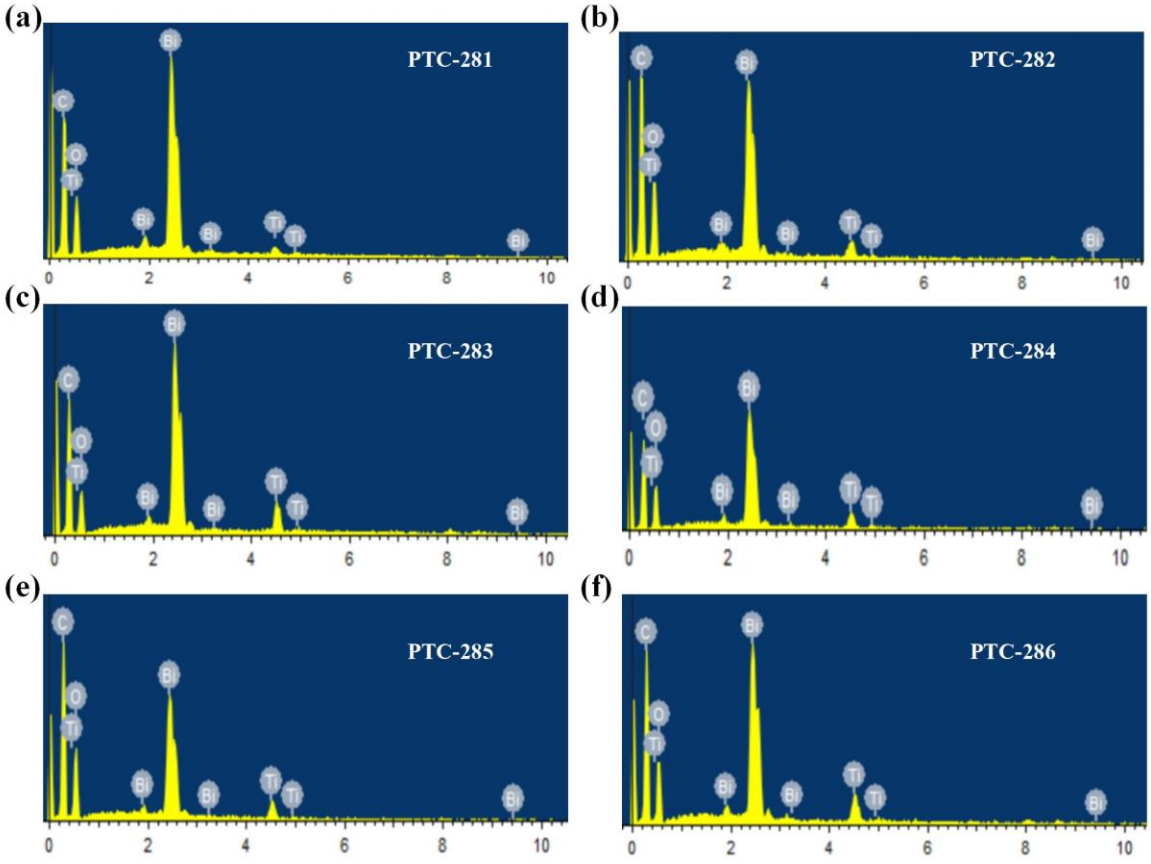

Figure S19. The EDS results of **PTC-284** to **PTC-286.**

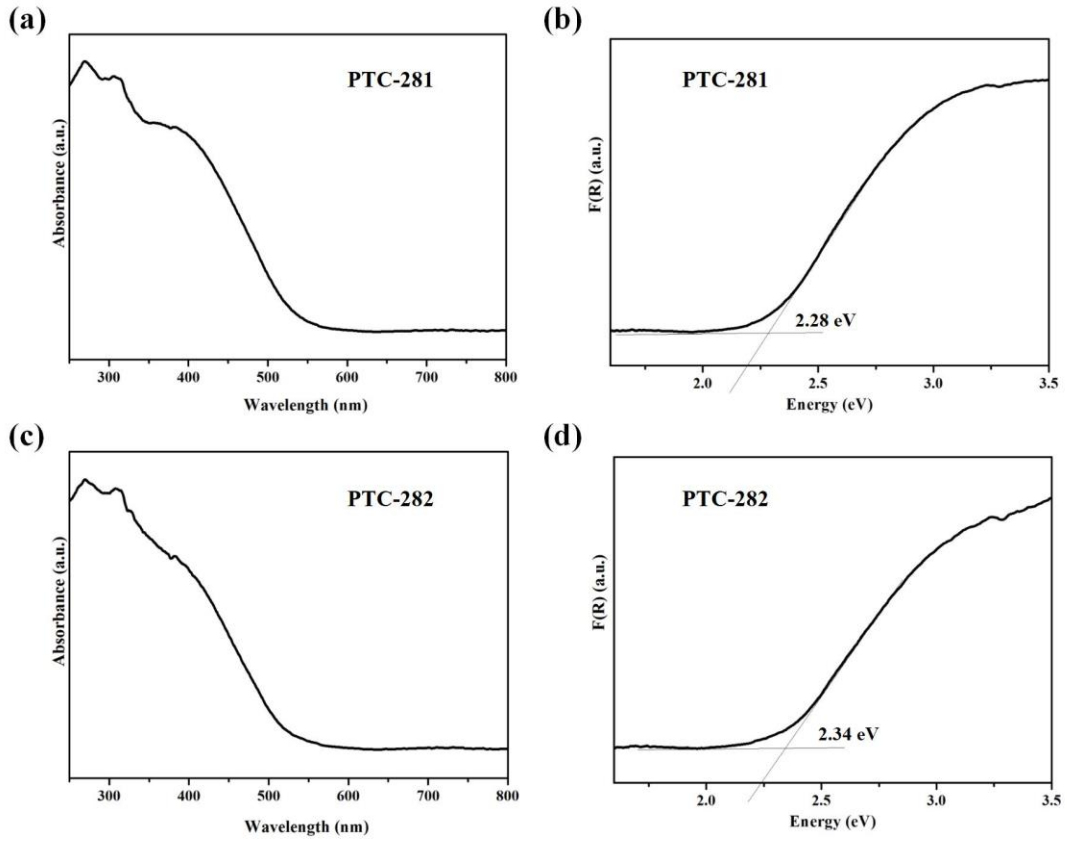

Figure S20. The absorption and bandgap spectra of **PTC-281** and **PTC-282.**

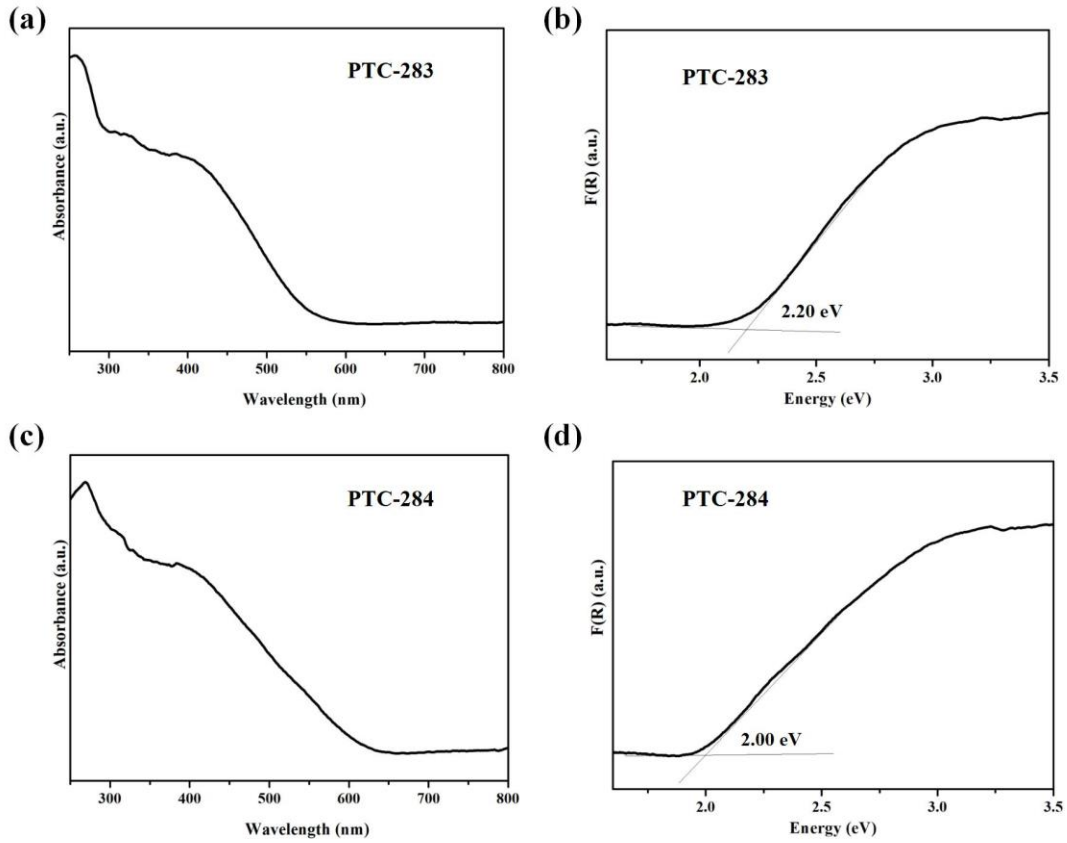

Figure S21. The absorption and bandgap spectra of **PTC-283** and **PTC-284.**

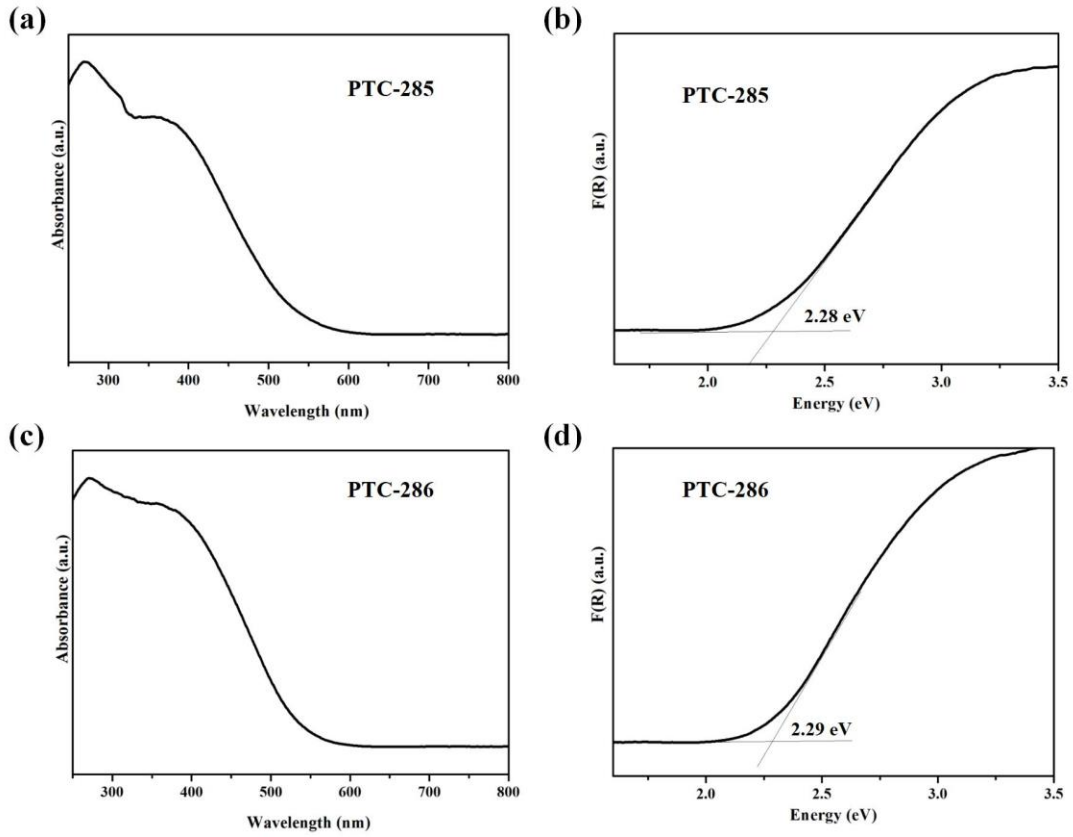

Figure S22. The absorption and bandgap spectra of **PTC-285** and **PTC-286.**

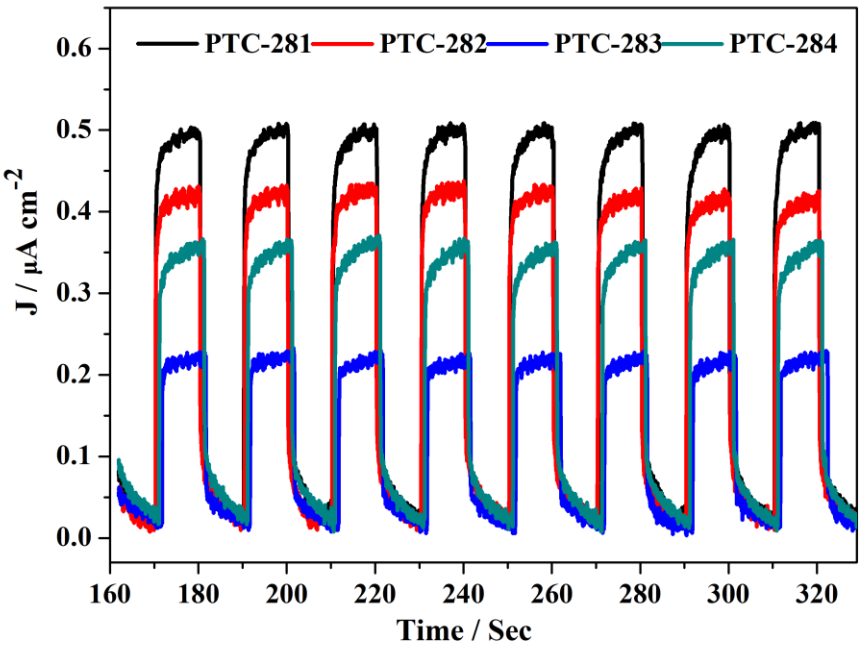

Figure S23. Transient photocurrent responses of **PTC-281** to **PTC-284** irradiated by visible light in 0.2 M Na_2SO_4 electrolyte solution.

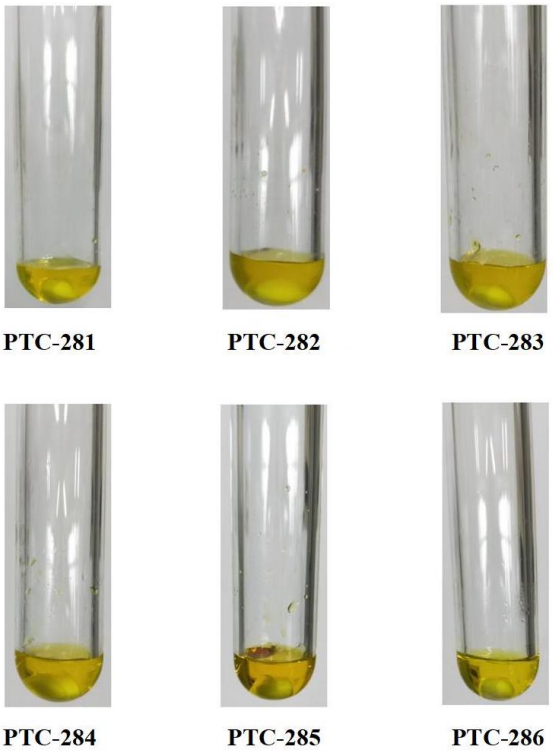

Figure S24. Photos of all samples after the catalytic reaction. Reaction conditions: 10 mmol epichlorohydrin, 0.005 mmol catalysts, 1 mmol nBu_4NBr, CO_2 (1 atm gauge pressure) and room temperature, for 24 h.

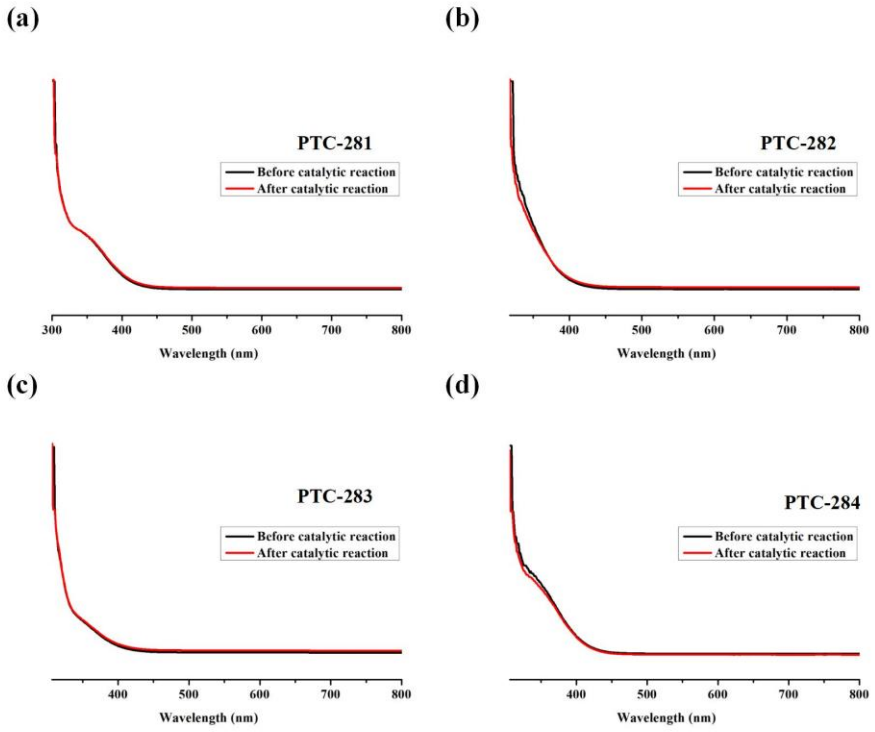

Figure S25. The solution-state UV-vis spectra of **PTC-281** to **PTC-284** before and after catalytic reaction. Reaction conditions: 10 mmol epichlorohydrin, 0.005 mmol catalysts, 1 mmol nBu_4NBr, CO_2 (1 atm gauge pressure) and room temperature, for 24 h.

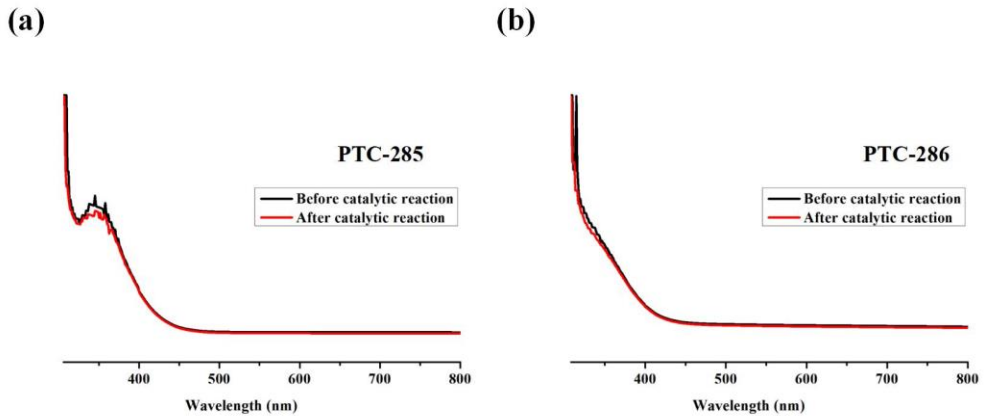

Figure S26. The solution-state UV-vis spectra of **PTC-285** and **PTC-286** before and after catalytic reaction. Reaction conditions: 10 mmol epichlorohydrin, 0.005 mmol catalysts, 1 mmol nBu_4NBr, CO_2 (1 atm gauge pressure) and room temperature, for 24 h.

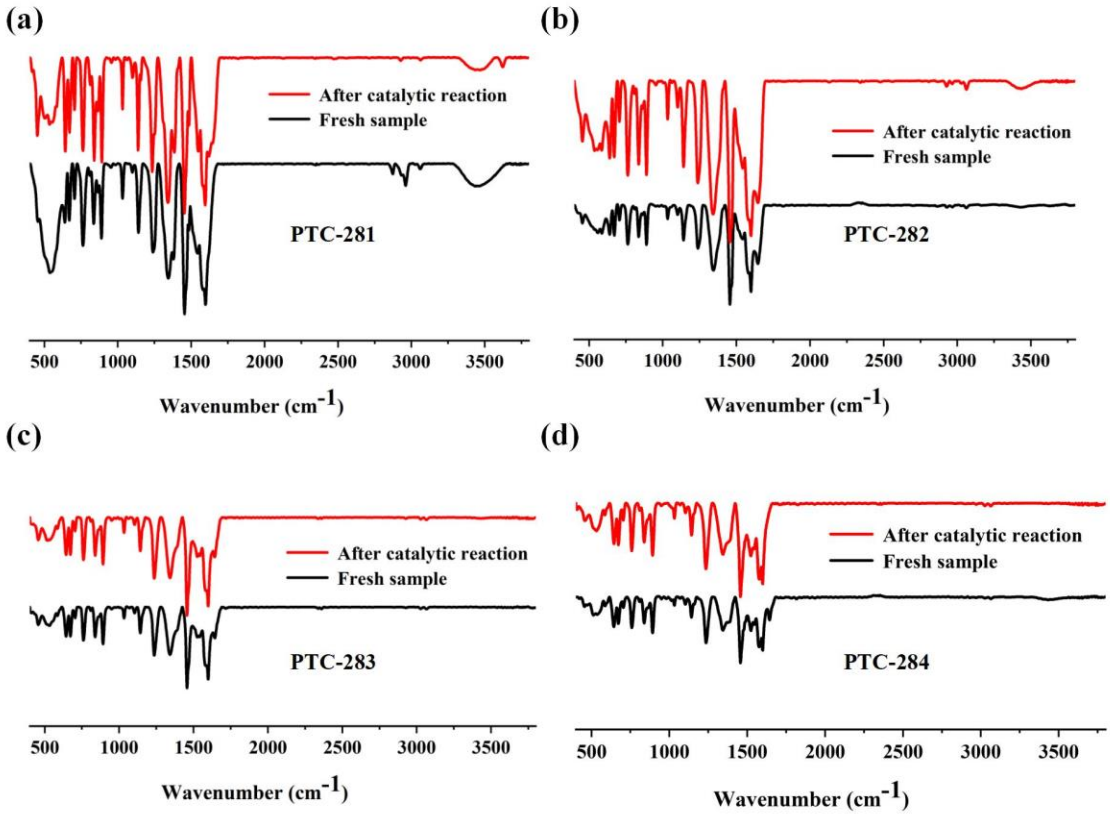

Figure S27. The solid-state IR spectra of **PTC-281** to **PTC-284** before and after catalytic reaction. Reaction conditions: 10 mmol epichlorohydrin, 0.005 mmol catalysts, 1 mmol nBu_4NBr, CO_2 (1 atm gauge pressure) and room temperature, for 24 h.

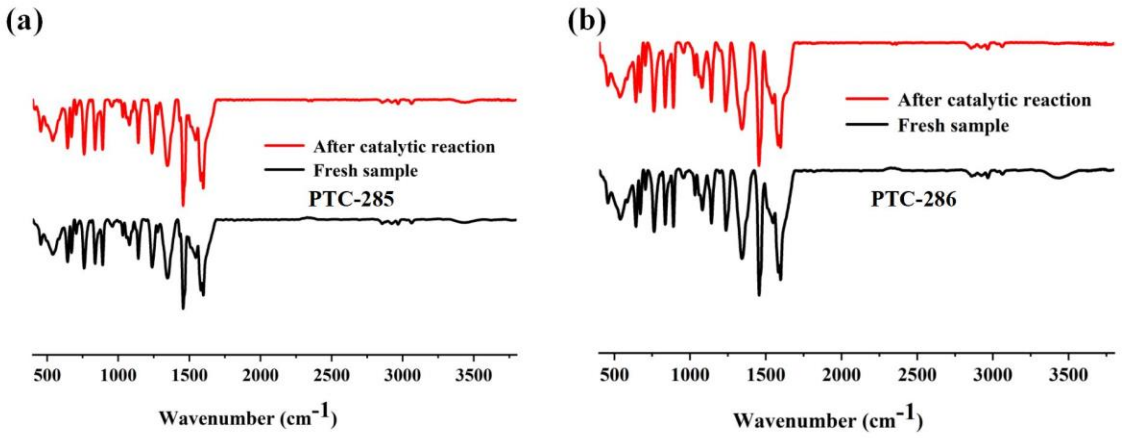

Figure S28. The solid-state IR spectra of **PTC-285** and **PTC-286** before and after catalytic reaction. Reaction conditions: 10 mmol epichlorohydrin, 0.005 mmol catalysts, 1 mmol nBu_4NBr, CO_2 (1 atm gauge pressure) and room temperature, for 24 h.

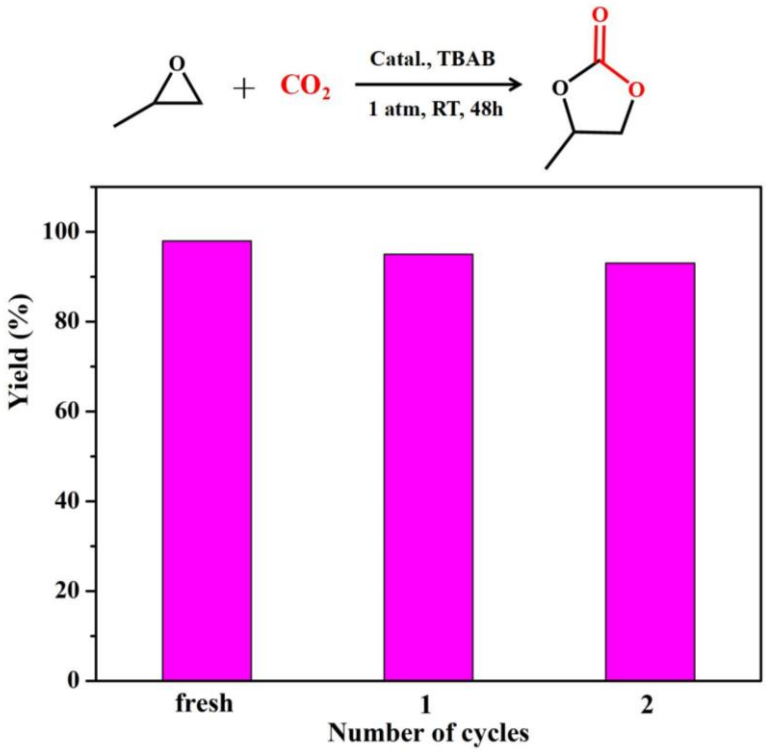

Figure S29. Recyclability of the **PTC-285** catalyst. Reaction conditions: 10 mmol propylene oxide, 0.005 mmol catalysts, 1 mmol nBu_4NBr, CO_2 (1 atm gauge pressure) and room temperature, for 48 h.

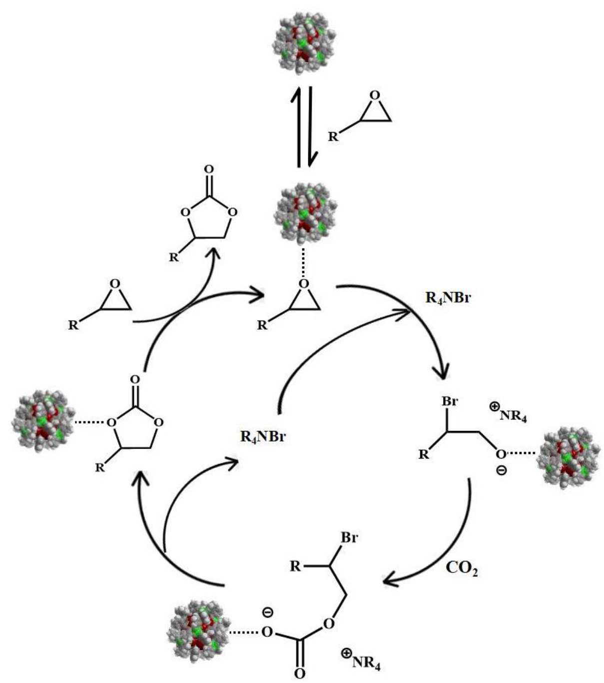

Figure S30. Proposed mechanism for cycloaddition of epoxides with CO_2 catalyzed by $Bi_{38}O_{44/45}$@Ti_xL-oxo core-shell clusters.

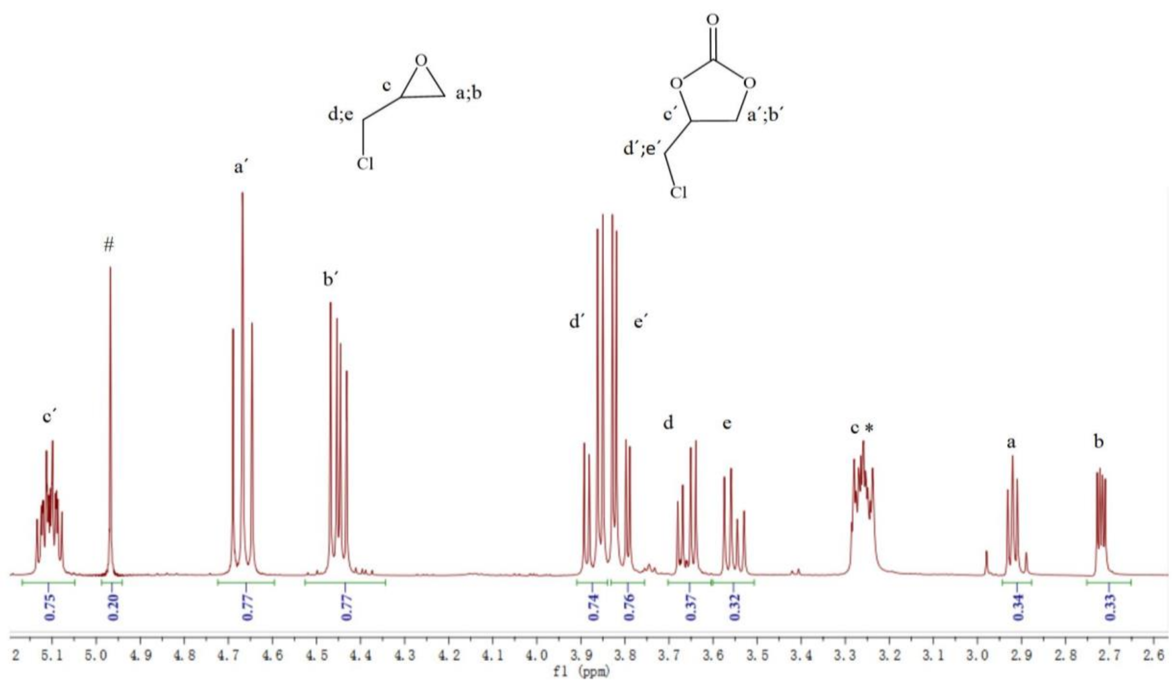

Figure S31. [1]H NMR spectra after 24 h CO_2 cycloaddition reaction of epichlorohydrin with **PTC-281** as catalyst. Peaks marked with * are for TBAB, with # is for CH_2Br_2.

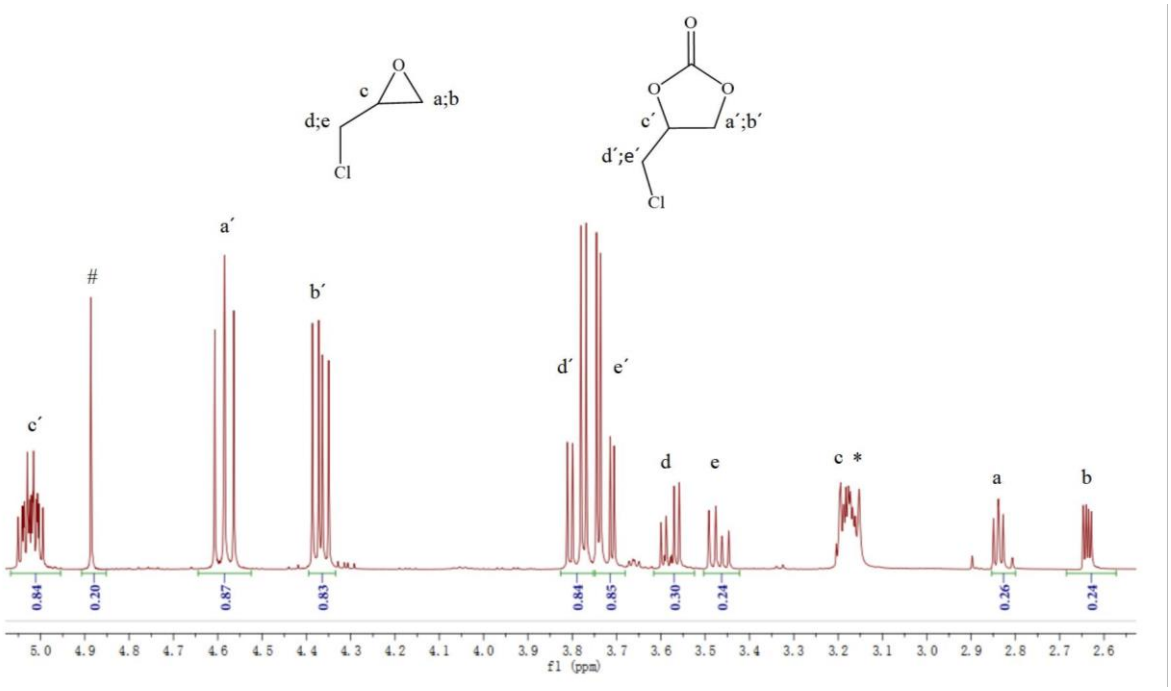

Figure S32. ^{1}H NMR spectra after 24 h CO_2 cycloaddition reaction of epichlorohydrin with **PTC-282** as catalyst. Peaks marked with * are for TBAB, with # is for CH_2Br_2.

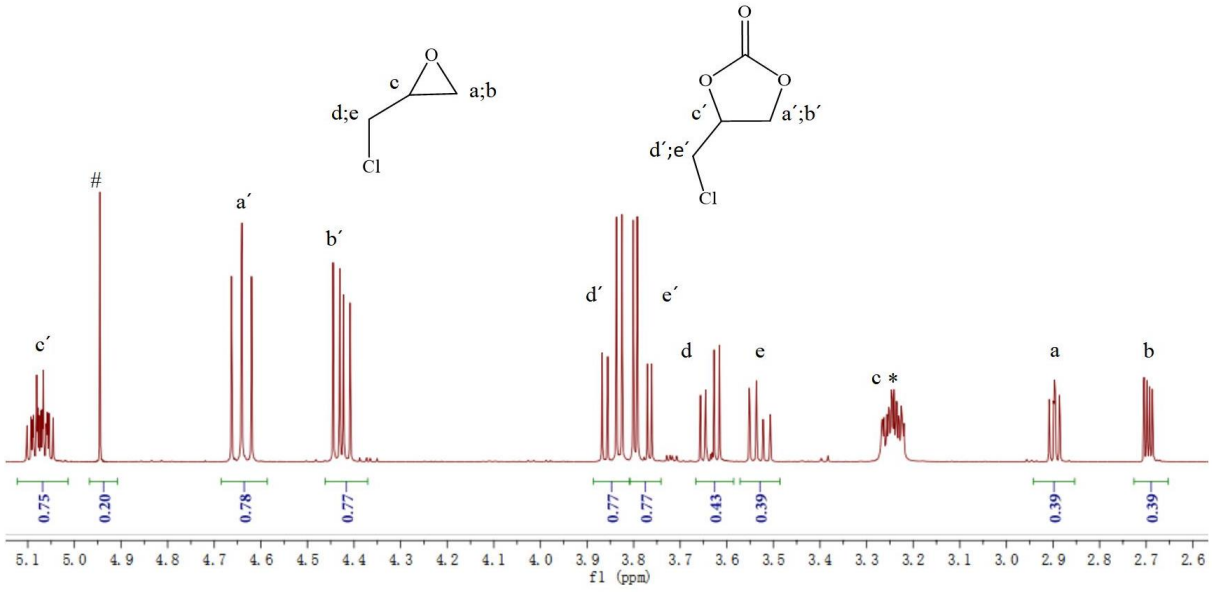

Figure S33. ^{1}H NMR spectra after 24 h CO_2 cycloaddition reaction of epichlorohydrin with **PTC-283** as catalyst. Peaks marked with * are for TBAB, with # is for CH_2Br_2.

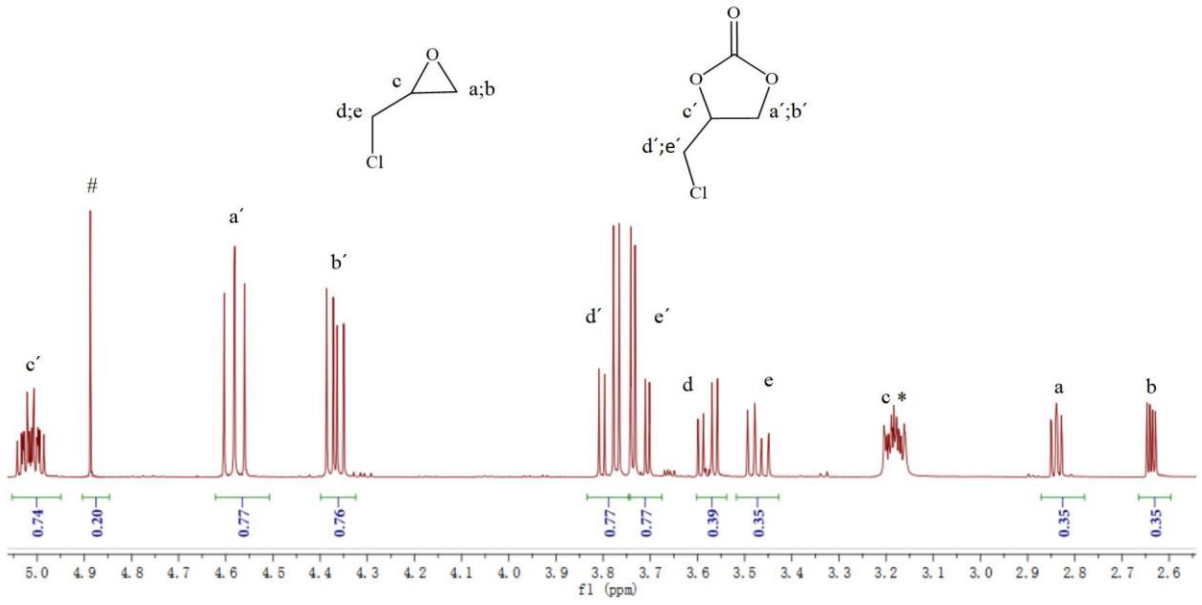

Figure S34. ^{1}H NMR spectra after 24 h CO_2 cycloaddition reaction of epichlorohydrin with **PTC-284** as catalyst. Peaks marked with * are for TBAB, with # is for CH_2Br_2.

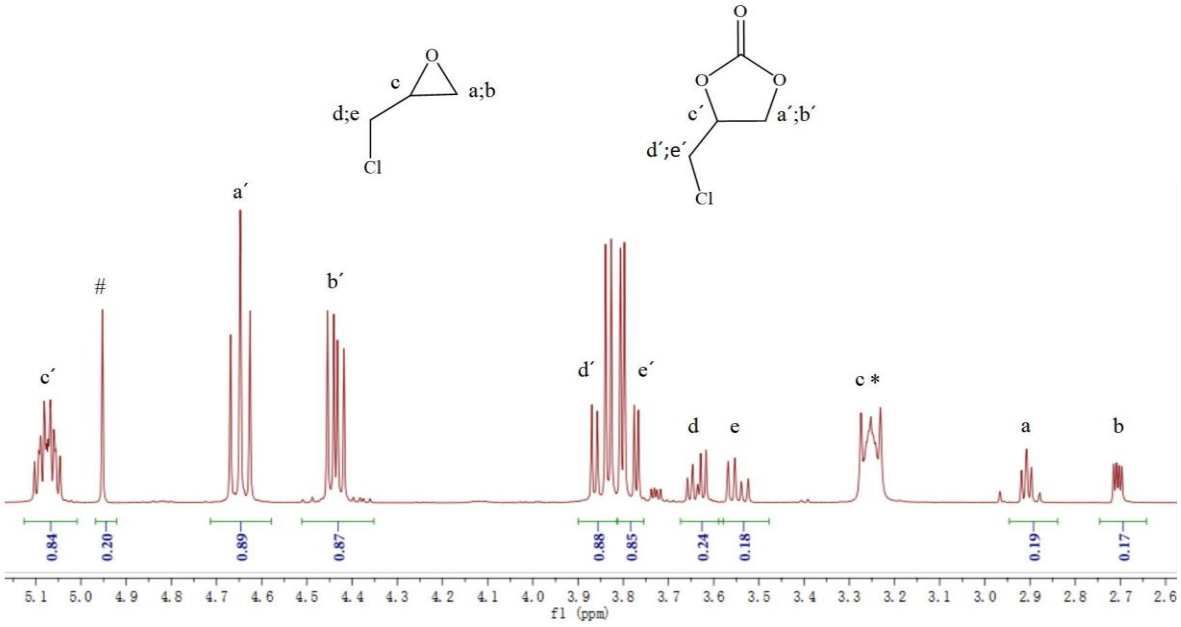

Figure S35. ^{1}H NMR spectra after 24 h CO_2 cycloaddition reaction of epichlorohydrin with **PTC-285** as catalyst. Peaks marked with * are for TBAB, with # is for CH_2Br_2.

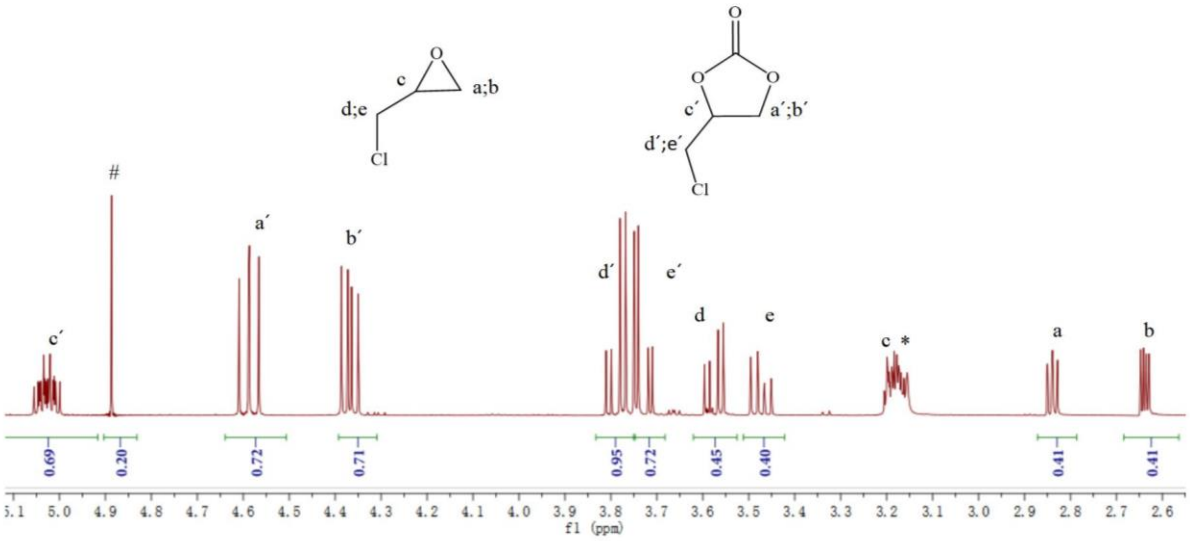

Figure S36. ^{1}H NMR spectra after 24 h CO_2 cycloaddition reaction of epichlorohydrin with **PTC-286** as catalyst. Peaks marked with * are for TBAB, with # is for CH_2Br_2.

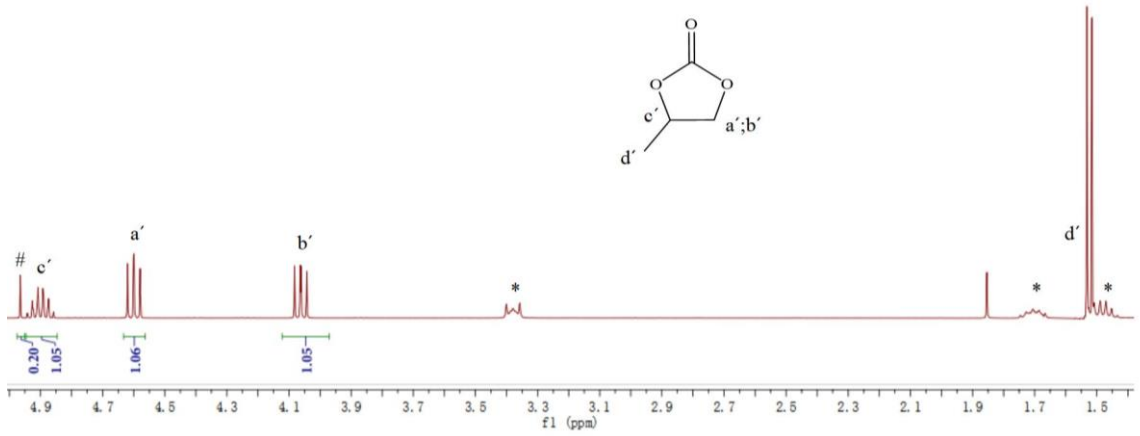

Figure S37. ^{1}H NMR spectra after 48 h CO_2 cycloaddition reaction of propylene oxide with **PTC-285** as catalyst. Peaks marked with * are for TBAB, with # is for CH_2Br_2.

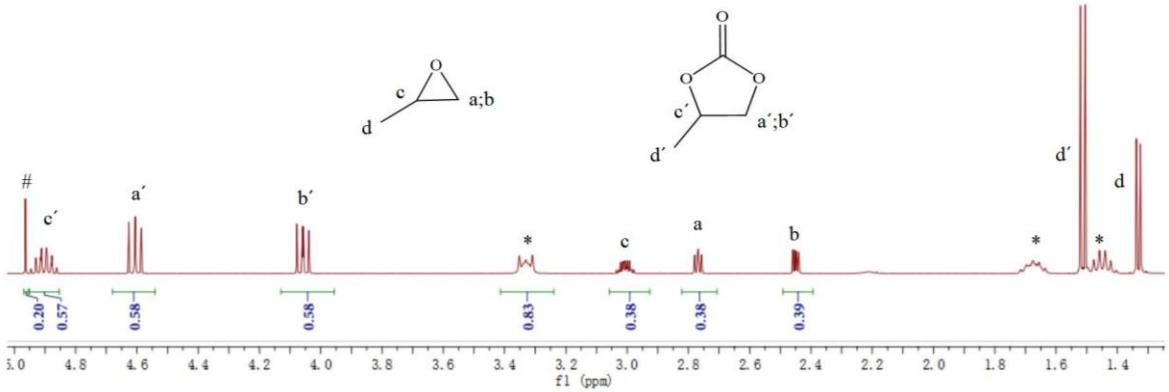

Figure S38. ^{1}H NMR spectra after 48 h CO_2 cycloaddition reaction of propylene oxide with **PTC-286** as catalyst. Peaks marked with * are for TBAB, with # is for CH_2Br_2.

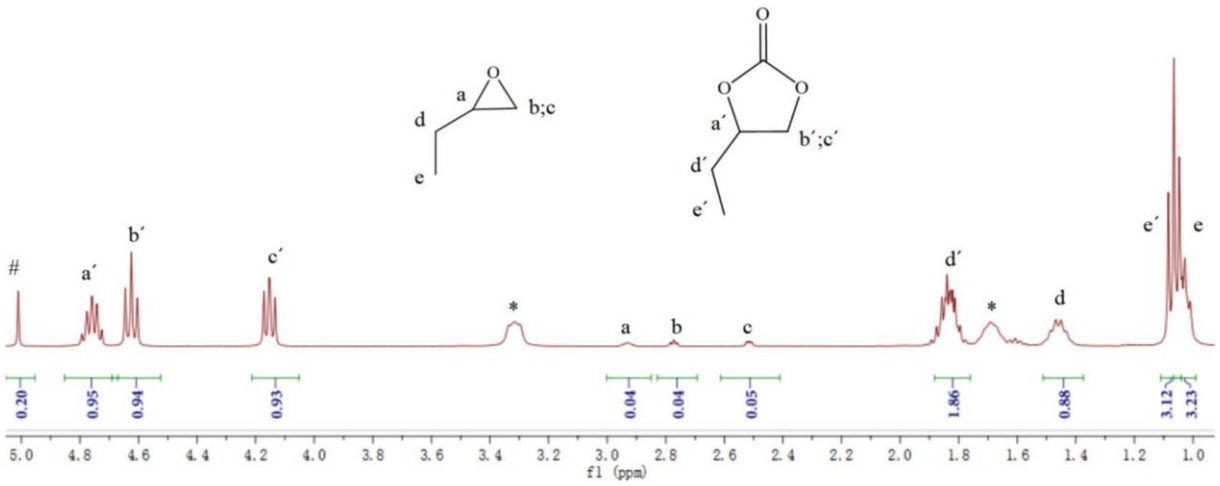

Figure S39. ^{1}H NMR spectra after 48 h CO_2 cycloaddition reaction of 1,2-epoxybutane with **PTC-285** as catalyst. Peaks marked with * are for TBAB, with # is for CH_2Br_2.

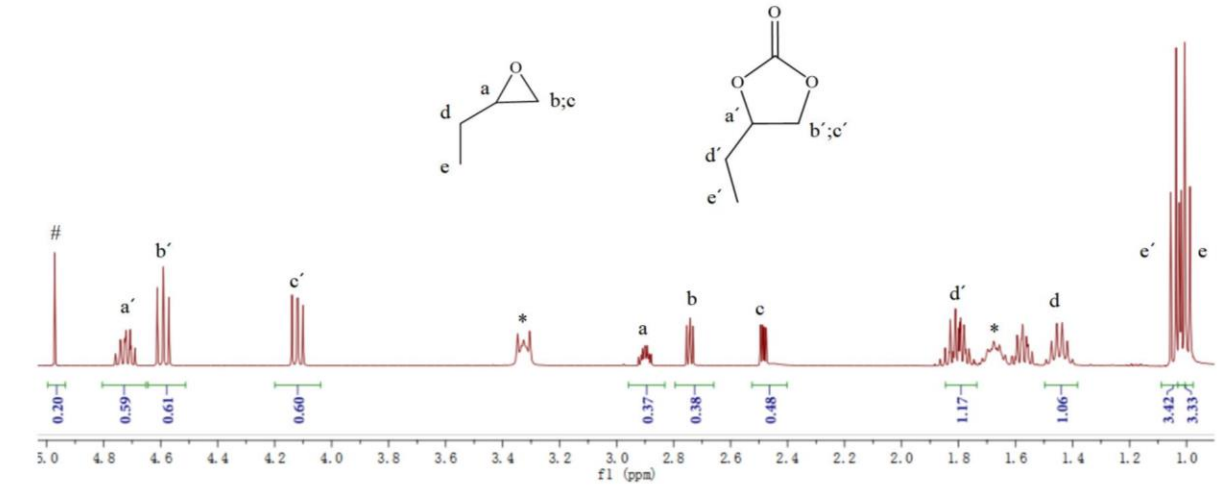

Figure S40. ^{1}H NMR spectra after 48 h CO_2 cycloaddition reaction of 1,2-epoxybutane with **PTC-286** as catalyst. Peaks marked with * are for TBAB, with # is for CH_2Br_2.

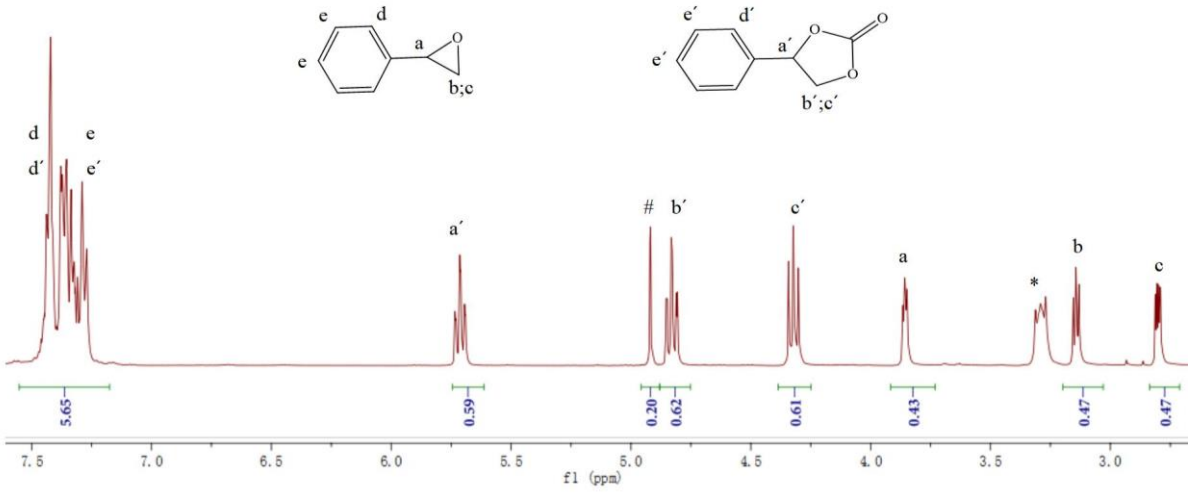

Figure S41. ^{1}H NMR spectra after 48 h CO_2 cycloaddition reaction of styrene oxide with **PTC-285** as catalyst. Peak marked with * is for TBAB, with # is for CH_2Br_2.

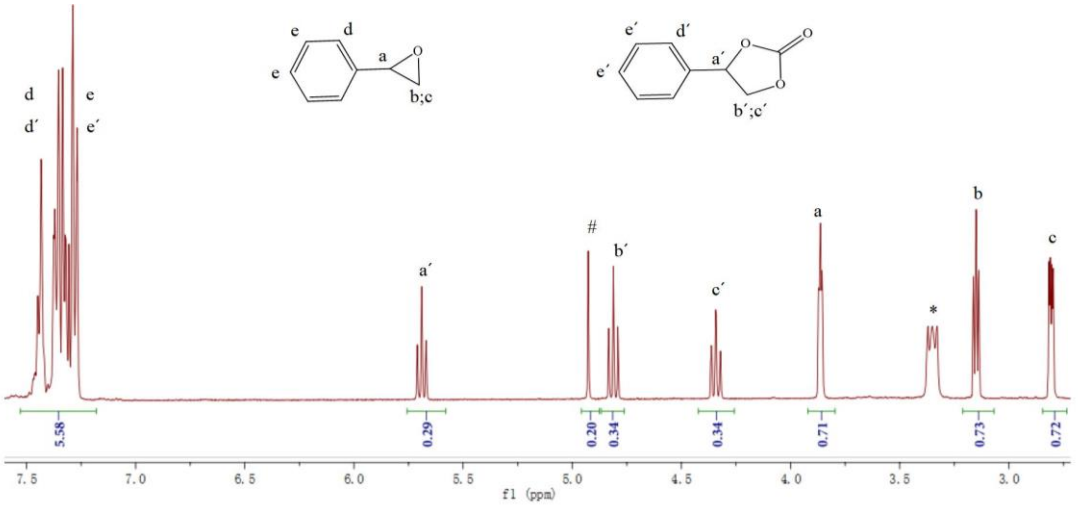

Figure S42. ^{1}H NMR spectra after 48 h CO_2 cycloaddition reaction of styrene oxide with **PTC-286** as catalyst. Peak marked with * is for TBAB, with # is for CH_2Br_2.

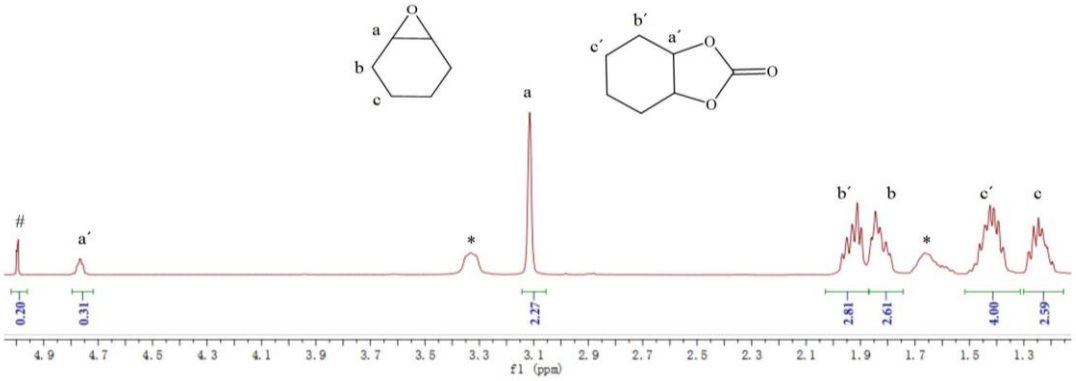

Figure S43. ^{1}H NMR spectra after 48 h CO_2 cycloaddition reaction of cyclohexene oxide with **PTC-285** as catalyst. Peaks marked with * are for TBAB, with # is for CH_2Br_2.

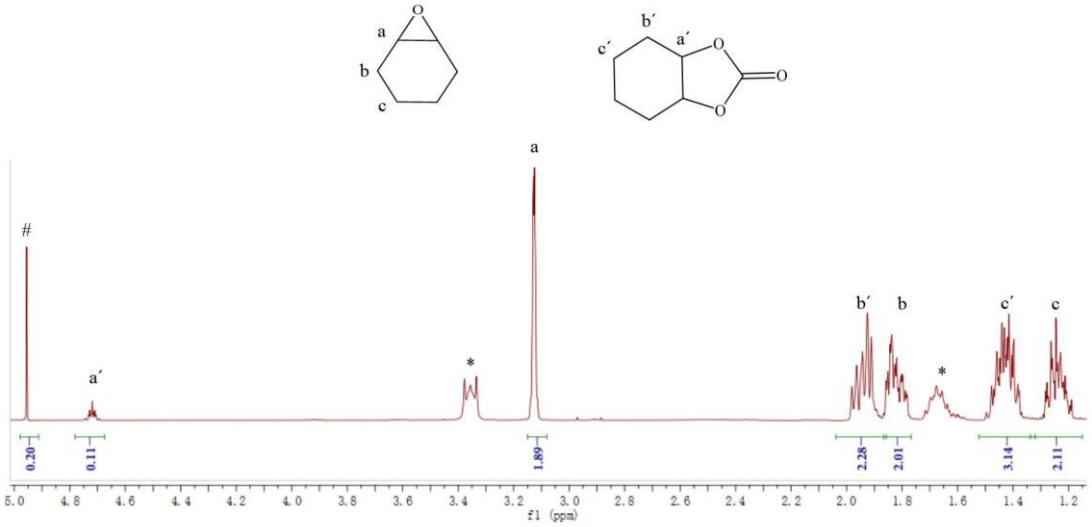

Figure S44. ^{1}H NMR spectra after 48 h CO_2 cycloaddition reaction of cyclohexene oxide with **PTC-286** as catalyst. Peaks marked with * are for TBAB, with # is for CH_2Br_2.

Table S6. The summary of the conversion of CO_2 and epoxides by some typical cluster catalysts and Bi -based materials

No.	Compounds	Co-catalysts	T (°C)	P (MPa)	t (h)	Yield (%)	Ref.
1	**PTC-285**	TBAB 10 mol%	r. t.	0.1	48	99	This work
2	$Au_{19}Ag_4(S\text{-}Adm)_{15}$	TBAB 10 mol%	60	2	24	85	[6]
3	$Tb_2Zn_2(\mu_3\text{-}OH)_2L_4(NO_3)_4$	TBAB 7.2 mol%	r. t.	0.1	48	99	[7]
4	$Zn_4(OCOCF_3)_6O$	TBAI 3 mol%	25	0.1	6	94	[8]
5	Hexanuclear Ti-oxo cluster	TBAI 16 mol%	80	10	18	79	[9]
6	Bismuth methoxide	LiI 0.48 mol%	r. t.	1	24	98	[10]
7	Bi(III) porphyrin	TBAI 2.4 mol%	90	2	1	92.9	[11]
8	Cationic Bi(III) complex	TBAB 0.0125 mol%	120	3	1	97.5	[12]
9	Binuclear Bi(III) complex	TBAI 0.10 mol%	140	3	1	97.5	[13]
10	Bi-PCNN-224	TBAI 1.66 mol%, light irradiation	r. t.	1	6	99	[14]

References

(6) G. Li, X. Sui, X. Cai, W. Hu, X. Liu, M. Chen, Y. Zhu, *Angew. Chem. Int. Ed.* 2021, **60**, 10573 -10576.

(7) R. Zhang, L. Wang, C. Xu, H. Yang, W. Chen, G. Gao, W. Liu, *Dalton Trans.*, 2018, **47**, 7159-7165.

(8) Y. Yang, Y. Hayashi, Y. Fujii, T. Nagano, Y. Kita, T. Ohshima, K. Mashima, *Catal. Sci. Technol.* 2012, **2**, 509.

(9) S. Kim, D. Sarkar, Y. Kima, M. H. Park, M. Yoon, Y. Kim, M. Kim, *J. Ind. Eng. Chem.* **2017**, **53**, 171-176.

(10) S.-F. Yin, S. Shimada, *Chem. Commun.* 2009, **9**, 1136-1138.

(11) J. Peng, Y. Geng, H.-J. Yang, W. He, Z. Wei, J. Yang, C.-Y Guo, *Molecular Catalysis.*, **2017**, **432**, 37-46.

(12) X. Zhang, W. Dai, S. Yin, S. Luo, C. T. Au, *Front. Environ. Sci. Eng. China*, 2009, **3**, 32-37.

(13) R. H. Qiu, Z. G. Meng, S. F. Yin, X. X. Song, N. Y. Tan, Y. B. Zhou, K. Yu, X. H. Xu, S. L. Luo, C. T. Au, W. Y. Wong, *ChemPlusChem*, **2012**, 77, 404-410.

(14) G. Zhai, Y. Liu, L. Lei, J. Wang, Z. Wang, Z. Zheng, P. Wang, H. Cheng, Y. Dai, B. Huang, *ACS Catal.* 2021, **11**, 1988-1994.